Task-dependent Constraints on 3-D Head Posture During Gaze Shifts

Melike Zeynep Ceylan

A thesis submitted to the Faculty of Graduate Studies in
partial fulfillment of the requirements
for the degree of

Master of Arts

Graduate Programme in Psychology
York University
Toronto, Ontario

October 1999

0-612-43372-2

Task-dependent Constraints on 3-D Head Posture During Gaze Shifts

by

Melike Zeynep Ceylan

a thesis submitted to the Faculty of Graduate Studies of York University in partial fulfillment of the requirements for the degree of

MASTER OF ARTS

ABSTRACT

Donders' law dictates that during visually orienting movements, motor systems choose only one particular 3-D orientation for each 2-D pointing direction. Different sub-laws are known to govern different segments, e.g. Listing's law for the eye and the Fick strategy for the head, resulting in different orientation ranges. However, despite considerable research and speculation, it is not known what perceptual, motor, or mechanical factors dictate the choice between these laws. I have observed that when 10 human subjects performed head-free gaze shifts between visual targets while wearing pin-hole goggles, Donders' law of the head was still obeyed, but it switched from the normal Fick strategy to approximate Listing's law. Further variations of this paradigm showed that this was not due to mechanical effect or a loss of binocular vision. Moreover, a head mounted laser task that emulated the motor task requirements with normal vision showed that the choice of strategy for Donders' law was due to perceptual factors, but rather motor task requirements. Finally, Donders' law broke down in a similar task where head pointing was dissociated from gaze. I conclude that Donders' law of the head is implemented neurally within the gaze control system and is optimized for motor task requirements, such that the head can be influenced to approximate Listing's law when its motor task requirements resemble those of an eye.

ACKNOWLEDGEMENTS

Above all I would like to extend my greatest appreciation and thanks to my supervisor Dr. Doug Crawford who took a chance on me and nurtured my love of science. Under his guidance, and exposed to his continued perseverance in the pursuit of knowledge, I have come to understand the frustration and elation associated with scientific discovery.

Personally I would like to extend my deepest thanks to my officemates Eliana, Denise, and Michael for their help on many difficult subjects, both academic and personal. I would also like to thank my committee members, Dr. Laurence Harris and Dr. James Elder for their support and valuable suggestions. Dr. Harris provided me with much encouragement and expressed much excitement in regards to my subject of study. Dr. Elder supported and provided me with much insight and advice on the areas that needed clarification. Thank you all for your support and providing me with a wonderful Masters experience.

Finally, and most importantly, I would like to thank my family for their love and support, without which I would be lost. Anne, you always supported me unconditionally, enjoying with me the good times and raising my chin during the bad. Baba, you always encouraged me to explore. You provided me with a strong morale background, which has guided me and made me a strong person capable of doing and being anything I desire. Finally, Kaan you have never let me down, never judged or discouraged me, you make be proud to be your sister. I love you all and always will. Çok teşekkürler.

TABLE OF CONTENTS

LIST OF ILLUSTRATIONS

GENERAL GAZE CONTROL

Reorienting oneself in an environment is generally initiated by the direction of the line of sight from, for example, one object of interest to another (i.e. gaze shifting). Gaze shifts are typically accomplished through the cooperation of the head and the eye such that during the gaze movement (amplitude > 25°; Phillips et al, 1995; Tomlinson and Bahra, 1986a) both the head and the eye would move the line of sight towards the intended goal. In humans and monkeys, the amount of eye and head contribution to the overall gaze shift is varied for same amplitude (i.e. size) gaze movements, from one instance to another (Freedman and Sparks, 1996). Even though this may be the case, it has been suggested that gaze control does not simply consist of random assignments of eye and head movements, but rather the kinematics (i.e. velocity, amplitude, movement onset, and positions of the eye and head relative to each other) follow certain lawful relationships (Freedman and Sparks, 1997). It was reported that according to these lawful relationships, one could accurately predict amplitudes, velocities, latencies, and durations of gaze and its relative components, of eye and head (Freedman and Sparks, 1997). If such lawful relationships are manifested in the movement kinematics of gaze control, then one could extend this notion to predict the patterning of behavior.

The vestibular ocular reflex. Initially it was believed that the head control systems did not play a role in gaze shifts (Bizzi et al, 1971). It was reported that any contribution the head made to the gaze shift was cancelled out by a compensatory eye movement, with an amplitude (i.e. size) equal to the head movement, in the opposite direction of gaze. In other words, it was proposed that head-free gaze shifts were like head-fixed gaze shifts (i.e. just an eye movement), independent of the accompanying head movement (Goossens and Van Opstal, 1997). Since it was believed that the head did not contribute to gaze shifts (or if it did, it was not significant), this and subsequent studies regarding gaze control were performed on subjects whose heads were stabilized (head-fixed). This method, however, only studies eye movements (the oculomotor system) and ignores the head motor system, hence disregarding one of the fundamental aspect of natural gaze movements, that being the contribution of the head to the shifting of the line of sight.

The compensatory eye movement made in response to a head rotation is part of the vestibular ocular reflex (VOR), a gaze stabilization mechanism that ensures that the eye remains on target (i.e. prevents retinal slip) during a head movement by rotating the eyes by the same amplitude as the head movement but in the opposite direction. The organ that detects movements of the head and relays the signal to the eye muscles is the semicircular canals. The semicircular canals consist of a pair of three bony tubes filled with fluid oriented 90° to each other such that movement (or more specifically, rotational velocity) in any of the three dimensions is detected (Goldberg et al, 1991). The canals are the input to the three-neuron arc that comprises the VOR with the vestibular nerve, abducens nucleus, and oculomotor nucleus being the three-nuclei and the eye muscles the final output (Galiana, 1990).

Saccades and gaze shifts. Typically gaze shifts are composed of saccades, or rapid eye movements, and head movements. Studying the saccadic system has provided most of our insight into gaze control. For example, research on the saccadic system has determined much of the underlying physiology and kinematics that govern eye movements.

The saccadic system is comprised of the physical plant (the eye, muscles, and surrounding tissue), brainstem, and cerebral structures. At its simplest, saccades are initiated by a "move" command and are told to stop and hold the desired target by a "hold" command. The "move" command is accomplished by a neural pulse signal that determines the speed of the eye movement and allows the eye to overcome muscle and tissue viscosity. The "hold" command is accomplished by a tonic step signal that counteracts the elasticity of the muscles, allowing the eye to remain on target. The generation of each of these signals is localized in the midbrain.

Physiological correlates of eye movements. The generation of saccades has its beginnings in the brainstem, more specifically at the level of the superior colliculus (SC). The SC is a laminated structure consisting of 7 layers, 3 superficial, 2 intermediate, and 2 deeper layers. The superificial layers receive direct inputs from the retina, and correspondingly neurons within these layers have specific visual receptive fields (Goldberg and Wurtz, 1972; Wurtz, Goldberg, and Robinson, 1982), which form a retinotopic map. At this level, the SC encodes the difference between where gaze is at the moment and where it will be redirected. Most animals and primates redirect the line of sight in order to foveate (i.e. direct the fovea, a highly densely packed area of the retina with the highest acuity) visual stimuli. When a stimulus of interest moves into the periphery of the eye, the SC encodes where gaze is at the moment (current retinal location or current gaze direction) and the location of the stimulus in the periphery (desired retinal location or desired gaze direction). The difference between the current and desired is termed retinal error. By redirecting the fovea (the line of sight) to the desired location, retinal error is reduced to zero as the fovea lines up with the stimulus.

Within the deeper layers of the superior colliculus, there is a motor map that lines up with the retinotopic map. When the head is fixed and neurons of this motor layer of the SC are stimulated with an electrical current, a saccade, with a specific amplitude (i.e. size) and direction, is elicited (Robinson, 1972). When the stimulation location is moved along the SC, saccades of different amplitudes and directions are also elicited. Therefore it was presumed that the deeper layer of the SC encoded saccades with respect to the rotation of the eye, more specifically, it encoded saccades in motor error coordinates.

The SC computes motor error as the difference between current eye position and desired eye position. Initially it was believed that the SC only coded motor error for saccades (Robinson and Jarvis, 1974). However, behavioral and modeling studies have reported that when the head is free to move, the signal coming out from the SC is not just a saccade motor error but rather a gaze motor error signal that directs gaze movements, i.e. the redirection of the line of sight (Galiana and Guitton, 1992; Galiana et al, 1992;

Tomlinson and Bahra, 1986). A stimulation study (Freedman et al, 1996) confirmed that in monkeys, when the SC is stimulated, a saccade is elicited, accompanied with a head movement. Similarly when the SC is stimulated in cats, there is a coordinated movement of the eyes and head (Harris, 1980). Results from a single-unit recording study on monkeys (Freedman and Sparks, 1997), which involved recording from neurons in the SC during gaze shifting, was also consistent with the finding that the SC encodes not just for saccades but also for head movements. These studies suggest that the SC outputs a gaze motor error signal that encodes both eye and head displacement.

Once the gaze motor error signal is generated by the superior colliculus, it is assumed that it decussates into separate saccade motor error (for eye movements) and head motor error signals (Freedman et al, 1996). However, as of yet it has not been determined where in the brainstem this occurs. Nevertheless, what is known is that the saccade motor error signal is sent to the burst generator where a pulse signal (a velocity command) is generated. The burst generator (i.e. the burst neurons) fires an intense burst of action potentials, which are linearly related to the amplitude of eye movement. For horizontal eye movements, the burst neurons are localized in the paramedian pontine reticular formation (PPRF; Lushei and Fuchs, 1972; Keller, 1974) and for vertical and torsional (i.e. about the line of sight) eye movements they are located in the rostral interstitial nucleus of the medial longitudinal fasciculus (riMLF; Buttner et al, 1977; King and Fuchs, 1979; Moschovakis et al, 1991, Crawford and Vilis, 1992). This pulse signal is then sent to the motoneurons, which synapse on the eye muscles and cause them to contract and subsequently move.

Another velocity related pulse signal is sent to an integrator, which calculates the static force required to keep the eye in the new position (i.e. desired position). The subsequent step signal (the static force) is relayed to the motoneurons, which in turn send a reduced sustained firing rate to the muscles for the length of time required for the eye to remain in this new position. The integrator for horizontal eye movements is found to lie in the brainstem in the nucleus hypoglossi prepositus (nPH; Cannon and Robinson, 1987), and for vertical and torsional eye movements, in the midbrain's interstitial nucleus of Cajal (INC; King et al, 1981; Fukushima, 1990; Crawford et al, 1991).

Physiological Correlates of head movements. The musculature and vertebrae involved in head movements is not as simple as for the eye. The eye plant can be described as a ball and socket comprised of the eye, the 6 muscles (*medial* and *lateral recti*, *superior* and *inferior recti*, and *superior* and *inferior obliques*), and surrounding tissue. The head, on the other hand, is much more complex in its action, i.e. multiple muscle activation and contention with gravitational and frictional forces (which the eye is not concerned with), and architecture. The head plant consists of the skull, up to 20 pairs of muscles, and several cervical and thoracic vertebrae (Richmond and Vidal, 1988). For sake of brevity, only the first 2 cervical vertebrae, atlas and axis, and major muscles will be discussed, since these are the most likely to be involved in head movements.

In humans, there are basically 3 types of head movements, each within the three orthogonal planes (Richmond and Vidal, 1988): flexion-extension (nodding), about the horizontal axis; lateral bending (ear to shoulder), about the torsional axis; and rotation (turning), about the vertical axis. The first two cervical vertebrae, the atlas and the axis, as well as the skull, play pivotal roles in each of the three types of movements. For example, the atlas and the axis form a pivot joint, the atlantoaxial junction, which has 2 degrees of freedom allowing movement around the vertical axis and limited movement about the horizontal axis. The joint formed by the skull and the atlas, the atlantooccipital joint, also has 2 degrees of freedom, movement about the horizontal axis and limited movement about the torsional axis.

The musculature pertinent to head movements are arranged in groups of layers. The outer group of muscles (*sternocleidomastoideus* and *trapezius*) connects the skull to the shoulder girdle, whereas the inner group (composed of long dorsal muscles: *splenius capitis*, *semispinalis capitis*, *longissimus capitis*; suboccipital muscles: *rectus capitis posterior major* and *minor*, *obliquus capitis superior* and *inferior*; and ventral muscles: *rectus capitis anterior major* and *minor*, *rectus capitis lateralis*) connects the skull to the vertebral column, and finally the innermost group (*splenius cervicis*, *longissimus cervicis*, and *semispinalis cervicis*) interlinks the vertebrae of the cervical and thoracic regions (Richmond and Vidal, 1988). Although it was believed that the larger muscles were responsible for turning, extending or flexing the head, and the shorter muscles for stabilization, the muscle activity associated with a particular head movement is much more complex. For example, to keep the head upright, only a few muscles are active. However when the head moves, several other neck muscles also become active depending on the speed and direction of movement, initial position of the head, loading, and the specific joints about which there is movement (Richmond et al, 1985).

The physiological structures involved in generating head movements are not as well understood as the saccadic system. Although it is has been shown that the superior colliculus, when stimulated, invokes head movements, it has been shown that these movements are coupled with saccadic movements for the purpose of redirecting gaze (Freedman and Sparks, 1997b). The structure responsible for the decussation of the gaze error signal, arising in the SC, into separate saccade and head motor errors are not as of yet been identified. However, a preliminary study performed on monkeys (Klier et al, 1999) has shown that when the vertical/torsional integrator for eye position (Interstitial nucleus of Cajal, INC) is stimulated, torsional head movements, in addition to torsional eye movements, are elicited. This would suggest that the INC is involved not just in eye movements, but also head movements. The question then arises as to whether INC integrates eye position and head posture signals separately, or does it integrate a single common gaze position signal. Results from the same study suggest that the INC integrates head posture separately from eye position because the signal is not integrated using the same coordinates as for eye movements (Listing's coordinates; Crawford et al, 1991; Crawford, 1994), but in another set of coordinates (Fick coordinates) consistent with behavioral observations (Glenn and Vilis, 1992; Radau et al, 1994). This would suggest that the INC is integrating separate eye and head signals. If this is found to be true, then the gaze motor error signal originating from the SC must decussate upstream from the INC. Several deep cerebellar nuclei (rostral and caudal fastigial nuclei, rFN and cFN) downstream from the SC and upstream from the INC have been postulated to be involved in gaze control (Goffart and Pelisson, 1998; Goffart et al, 1998) and are under study as possible structures for the bisection of the gaze motor error signal.

3-D GAZE CONTROL

Behavioral Coordinate Systems. When attempting to localize an object in three-dimensional space, for example a coffee cup, there are six variables that need to be defined: three for position, using Cartesian coordinates (x,y,z) for example; and three for orientation (pitch, yaw, and roll for example; Hollerbach, 1990). Although the coffee cup may occupy a certain position, it is a three-dimensional (3-D) object and as such can have an infinite number of orientations for each position.

How do researchers describe rotations of the eye or head? According to convention, the axis of rotation is specified when discussing rotations of the eye and head in humans and monkeys. For example, when someone nods their head up and down (i.e. pitch), the behavior is said to be a vertical movement about some horizontal axis (figure 1C). By expressing the movement as "vertical" and the axis "horizontal", an orthonormal coordinate system is being used. Once the coordinate system has been specified, the movement's direction can be quantified. This is typically accomplished with vectors. In this example, if the direction the nose is pointing is taken as the pointing direction, the pointing direction of the head at rest can be described as the reference position of the head (an arbitrary designation). With the reference position and axes of the coordinate system defined, it is possible to determine the amplitude of the movement by vector algebra by determining the angle of rotation from a reference position to the final position, about some fixed axis. For this example, assume that the head rotated upward

Figure 1

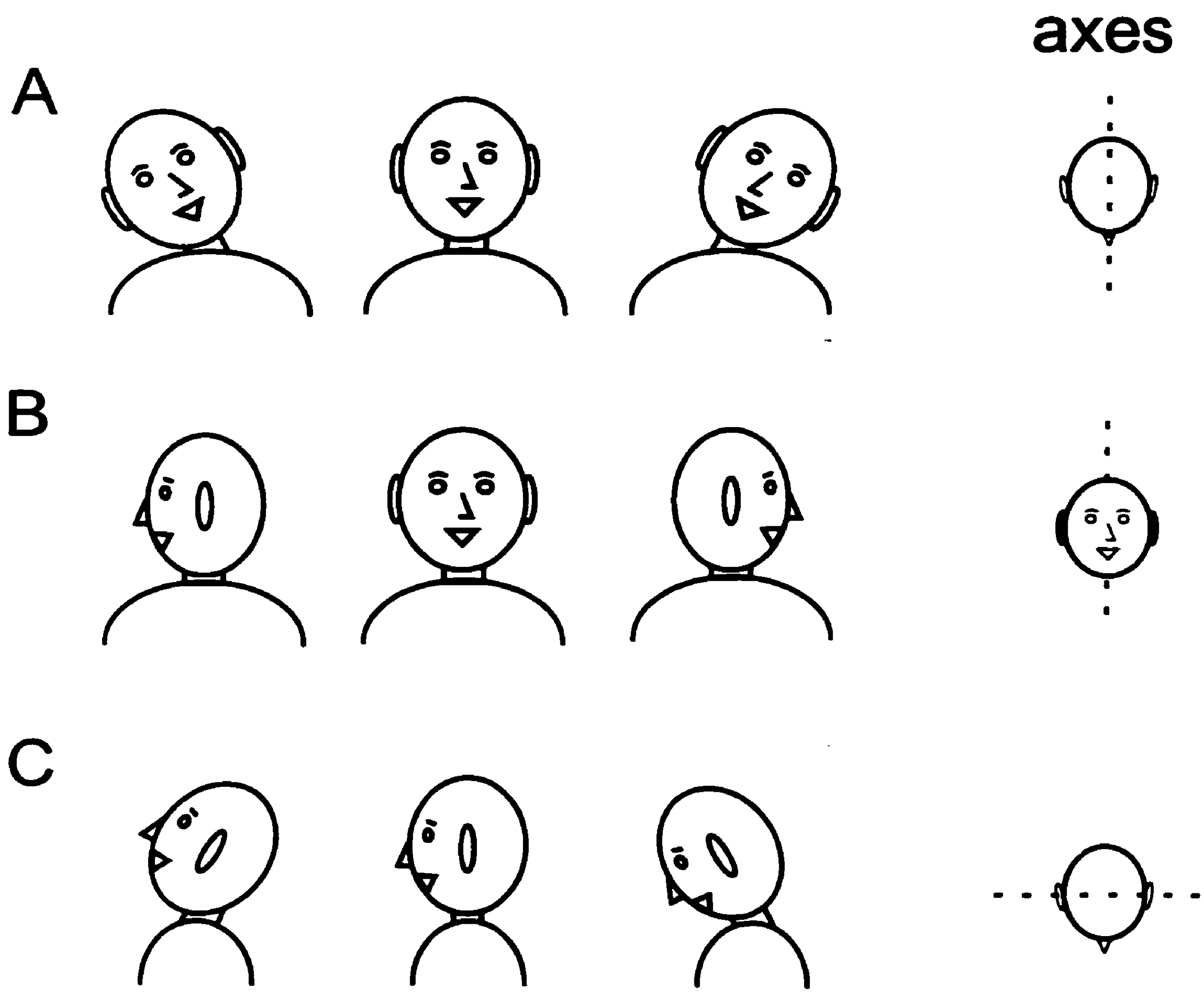

Figure 1. Three axes of rotation for the head. Axes are denoted by the dashed lines. ***A***: subject is viewed from the front; axis viewed from above the subject. Torsional head rotation about the torsional axis (i.e. about the gaze line). ***B:*** subject viewed from the front; axis viewed from the front of subject. Horizontal head rotation about the vertical axis. ***C:*** subject is viewed from the side; axis viewed from above the subject. Vertical head rotation about the horizontal axis.

by some amount. The angle between the current pointing direction (imagine a line emanating from the nose) and the reference position determines the amplitude (i.e. size) of the movement about the horizontal axis (upward rotations of the head are about the horizontal axis).

One coordinate system used in defining eye and head movements is the apparatus used to measure them. For example, an apparatus used to measure 3-D eye and head rotations is the 3-D magnetic search coil technique (Robinson, 1963; Ferman et al, 1987; Tweed et al, 1990; Tweed and Vilis, 1991). This technique involves having subjects sit in the middle of three mutually orthogonal magnetic field coils with a search coil inserted into the eye (to measure eye position), or a coil taped to a cap on the subject's head (for measuring head position). In figure 2, the subject would be positioned in the field such that the subject's sagittal plane is vertical and aligned with the vertical of the field. For the purposes of this study, the coordinates used to determine head positions relative to space is that that is aligned with the coils, henceforth referred to as coil coordinates. That is, the vertical axis of the head is aligned with the vertical coil, and so forth.

Many researchers in the area of eye and head motor control have defined rotations of the eye or the head, but have chosen not to specify translational position. The reason for this is, in the case of eye movements, eye position changes very minimally (i.e. the eye does not move around in the head, it rotates about some fixed axis of rotation). The head, in contrast, is capable of changing position, i.e. can translate. However, research has tended to focus on the rotational kinematics of the head and as such the role of

Figure 2

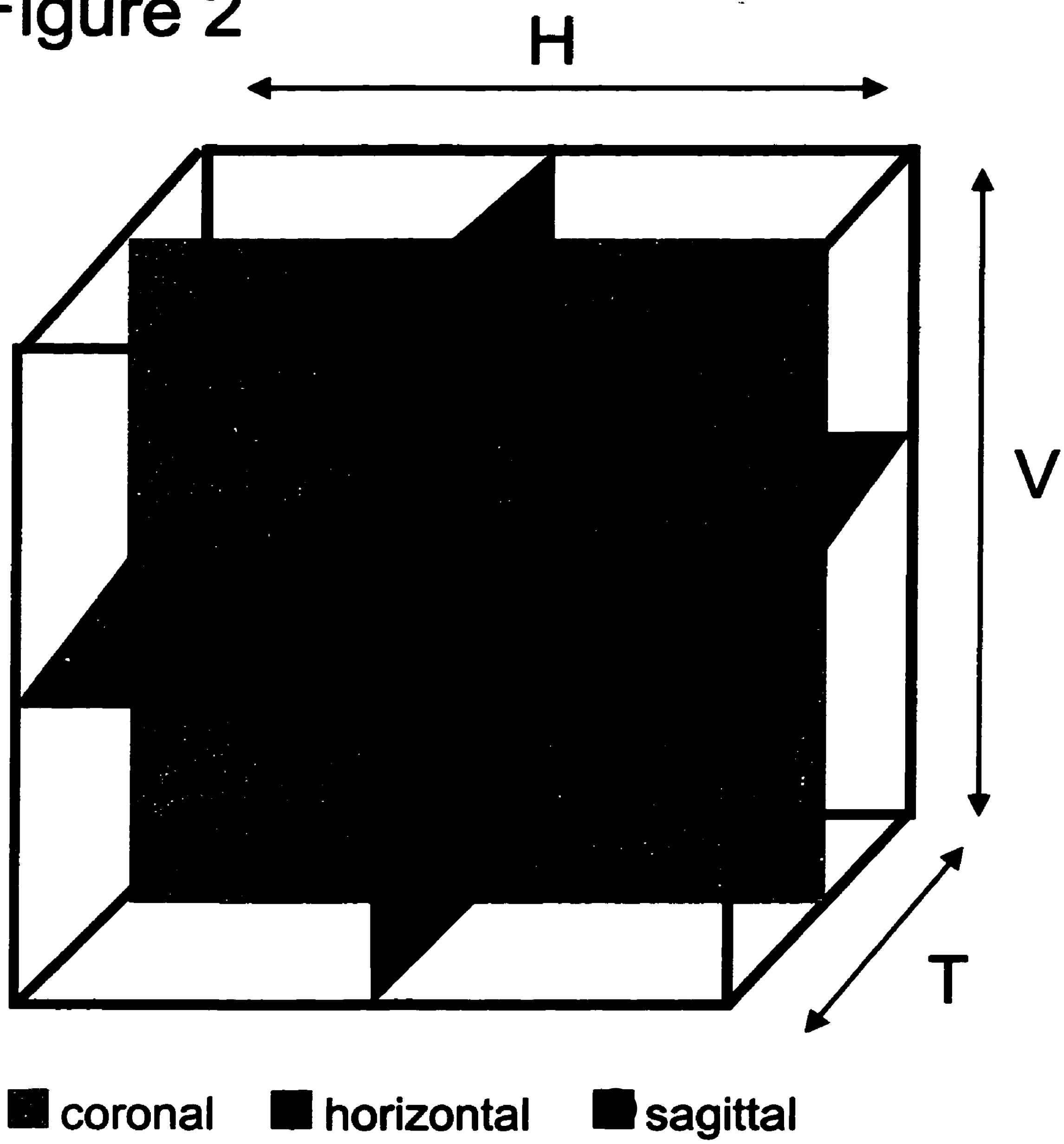

Figure 2. Schematic of the 3-D magnetic search coil system used in the study and the resulting coil coordinates used to express head movements. The cube is the physical layout of the magnetic field system with the following designations: *h* is the horizontal axis for vertical rotation; *v* is the vertical axis for horizontal rotation; *t* is the torsional axis for torsional rotation. A coil would be attached to the subject's head which would be in the middle of the three mutually orthogonal fields. The intersection of the saggital and coronal plane is aligned with the vertical of the field; the intersection of the horizontal and coronal plane is aligned with the horizontal axis of the field; and the intersection of the coronal and saggital plane is aligned with the torsional axis.

translational movements in understanding rotational kinematics has not been completely addressed (Glenn and Vilis, 1992; Radau et al, 1994; Crawford et al, 1999; Goffart and Pelisson, 1998; Straumann et al, 1991). This trend is shifting and the role of translation in determining the type of strategies adopted by the motor system in resolving problems (such as kinematic redundancy) is being realized (see Medendorp et al, 1998).

Kinematic redundancy and Donders'Law. The eye and the head are rotational systems capable of rotating in any of the three dimensions, vertical, horizontal, and torsional. Thus they are each said to possess three degrees of freedom. Gaze direction, on the other hand, is a two-dimensional (2-D) entity defined by vertical and horizontal directions. This gives rise to a difficult problem for the brain to solve since it has to specify a three-dimensional (3-D) eye orientation for a two-dimensional gaze direction, and a 3-D head orientation for a 2-D facing direction. To redirect gaze, then, the brain would have to specify a horizontal and vertical rotation for the eye that corresponds to the intended location of the target, and a horizontal and vertical rotation for the head that would best bring the eyes on target. However, the eye and head are also mechanically capable of rotating about the line of sight without affecting the direction of gaze. How then does the brain choose a specific torsional orientation for the eye and the head from an infinite number of possibilities? And why?

Donders, in the 19th century, provided a solution whereby when the head is held upright and fixed, 3-D eye orientation for a given gaze direction is always the same irrespective of where the eye came from (Donders, 1847). That is, the eye would always adopt the same orientation for a given gaze direction such that accumulation of torsion (rotation about the line of sight) would be minimal. By doing so, the system would potentially simplify the complexity associated with visual (2-D input) to motor (3-D output) transformation by restricting final eye position to a 2-D subspace of the 3-D space of all possible orientations (Helmholtz, 1867; Ferman et al, 1987; Tweed and Vilis, 1990; Straumann et al, 1991; Hore et al, 1992). This constraint is known as Donders' law and has been extended to apply to any motor system that has a redundant degree of freedom that needs to be eliminated (i.e. head motor system, arm motor system involved in pointing, etc) in accordance with skeletomuscular constraints (Ferman et al, 1987; Tweed and Vilis, 1990; Straumann et al, 1991; Glenn and Vilis, 1992; Hore et al, 1992; Radau et al, 1994; Crawford et al, 1999).

What are the advantages of Donders' law besides reducing complexity? Donders' law, as one would expect, prevents the accumulation of torsion (rotation about the torsional axis). If a rotating body, like the eye, head, or arm, did not obey Donders' law, there would be the potential for the accumulation of torsion. This would be undesirable in the above stated cases since the musculature involved in rotating and supporting the eye, head, or arm has mechanical limits that would be violated (Hore et al, 1992; Radau et al, 1994). That is, the eye, arm, or head does not have the mechanical capability to rotate about a torsional axis continuously without some "reset" mode that would bring it back to its natural resting position. Thus Donders' law seems to be in place to ensure that the limits are not exceeded. As well, when the system is not concerned with the accumulation of torsion (i.e. accumulated rotation about the torsional axis), it is not obeyed. For instance in a study by Tweed and Vilis (1992), when head orientations were measured after subjects made repetitive gaze shifts between 2 horizontal targets, Donders' law was abandoned for a more efficient minimal rotation strategy. Torsion in this case does not accumulate since the minimal rotation strategy requires only one axis of rotation and any torsion accumulated is cancelled out.

Listing's Law. Although the oculomotor, head motor, and arm motor systems have been reported to adhere to Donders' law, the implementation of the law is quite different in each motor system. Initially, Listing and Helmholtz in the 19th century focused on the oculomotor system and attempted to describe the amount of torsion assigned at each final eye position, i.e. Donders' unique orientation (Helmholtz, 1867). To accomplish this, they needed to specify a particular eye position and express final eye positions as single rotational displacements from this position. The corresponding axes of rotation by which the eye rotated from this particular position to the desired locations were found to lie in a single plane (figure 3C). This particular position is termed primary position and is thus the only position where this plane is orthogonal to gaze direction. The plane, orthogonal to primary position, and roughly parallel with the coronal plane of the head (in both humans and monkeys, the plane can tilt away from the coronal plane; Tweed and Vilis, 1990), is called Listing's plane and is the 2-D subspace to which eye position is restricted to such that the angle of ocular torsion is null (Westheimer, 1957). Hence Listing's law states that the eye only assumes those positions that can be reached from primary position by a single rotation about an axis in Listing's plane (Tweed and Vilis, 1990). The existence and positioning of Listing's plane has been experimentally verified in human and monkey subjects through the advent of the 3-D search coil technique (Ferman, Collewijn, and Van den Berg, 1987; Tweed et al, 1990; Crawford and Vilis, 1991; Straumann, Haslwanter, Hepp-Reymond, and Hepp, 1991).

To demonstrate Listing's law, figure 3 plots model simulated final head orientations (instead of eye, for visual comparison with figure 4) that would be adopted if the head obeyed Listing's law (A) and the corresponding orientation vectors (plotted as quaternions) as viewed from the front (B) and the side (C) of the subject. Orientation vectors are vectorial representations of the rotational movement, specifying both direction (i.e. up/down, left/right, clockwise/counterclockwise) and amplitude (the tip of the vector represents final head position). Since these vectors are plotted using the quaterion method (see appendix), then by using the right-hand rule, the direction of the movement can be determined. In figure 3B, by pointing one's right thumb in the direction of orientation vector 1, it is determined that the movement was leftward since the fingers curled in the leftward direction. By examining the corresponding final head orientation (i.e. orientation 1) adopted in the simulation (A), relative to the starting head position

Figure 3

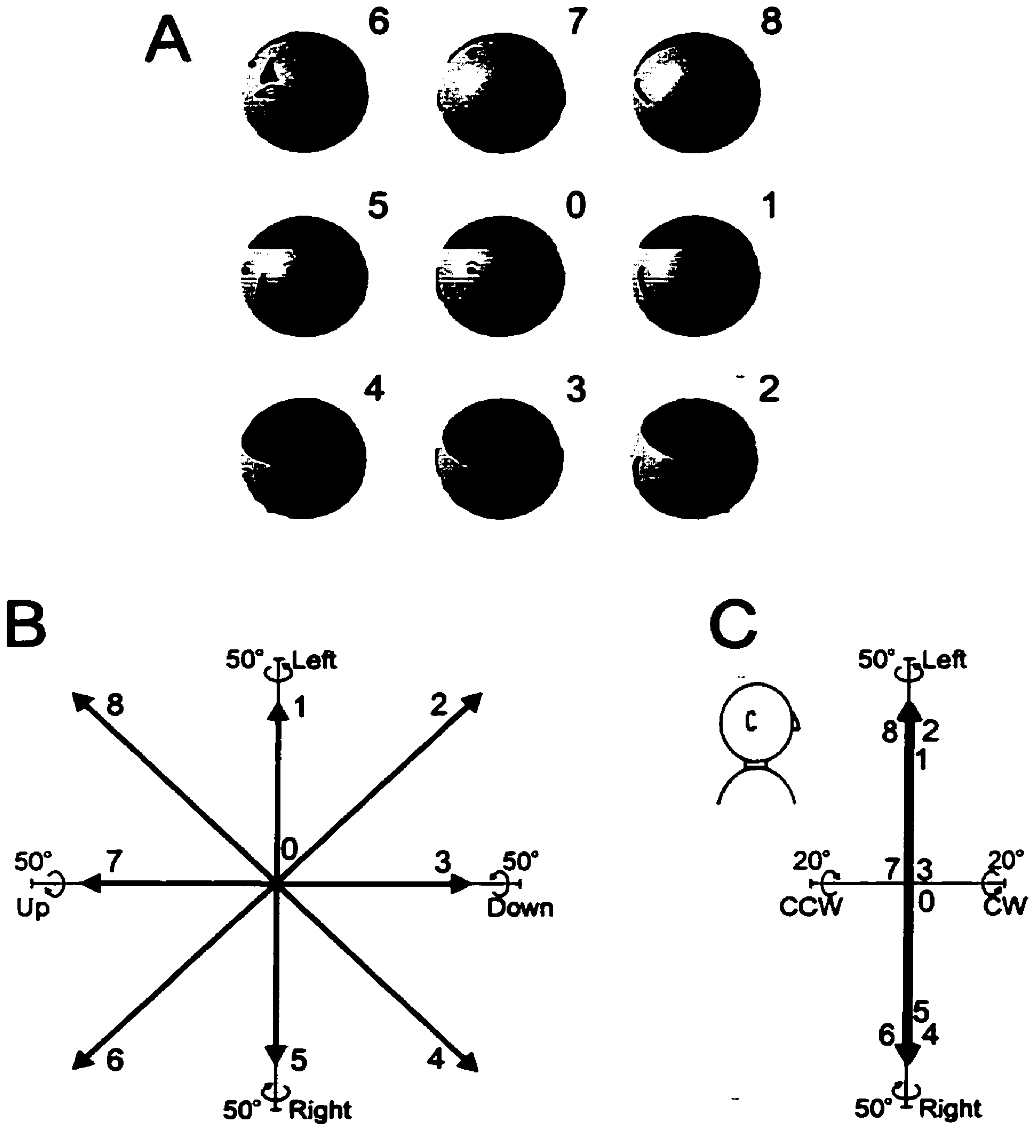

Figure 3. Hypothetical kinematics of a head obeying Listing's law. ***A:*** hypothetical final head positions assumed by rotation from center to each of the 8 targets used in the study (4, 40° up/down/left/right; 4, 48° oblique), viewed from the front. ***B:*** frontal (i.e. horizontal vs. vertical axes) projection of the distribution of head orientation vectors for final head positions in A plotted in space-fixed coordinates. Vectors are plotted as quaternions such that the right-handed rule applies, e.g. For position 1 in A, the right thumb would be pointed upward such that the fingers would curl leftward, in the direction of rotation (subject is viewed from the front in A, necessitating a flip in the horizontal axis, i.e. up is negative, down is positive). Orientation vectors are labeled with their corresponding number, e.g. 1 in B is the orientation vector for final head position 1 in A. ***C:*** same distribution of orientation vectors in B but viewed from the side (i.e. vertical vs. torsional axes). The space-fixed distribution of orientation vectors lie in a plane.

(orientation 0), it appears that the rotation was made to the left. If we examine these same orientation vectors from the side of the subject, they appear to lie in a flat plane, along the vertical axis. This plane is Listing's plane, and primary position would be orientation 0 in figure 3A since this orientation is orthogonal to the plane, and head orientations 1 through 8 were accomplished as single rotations from this position.

To describe rotations using Listing's law, it has been the norm to use Listing's coordinates where the vertical axis is orthogonal to primary position (and parallel with Listing's plane) with all three axes (vertical, horizontal and torsional) being mutually orthogonal. To fully localize eye positions, the reference frame used is the head since Listing's plane is fixed relative to the head. Several reasons for this convention is that it is presumed to be the most physiologically consistent (the semicircular canals and eye muscles are fixed relative to the head) and simplest to use (it rotates the data such that Listing's plane aligns with the vertical axis).

Much of the controversy associated with Listing's law of the eye deals with whether it is a neural (Crawford and Vilis, 1991; Haslwanter, Straumann, Hess, and Henn, 1992) or mechanical (Ferman et al, 1987; Schnabolk and Raphan, 1994) constraint. That is, is Listing's law implemented somewhere in the brain circuit or do the eye muscles themselves constrain final eye positions (Ferman et al, 1987; Schnabolk and Raphan, 1994). It is important to understand the implementation of Listing's law since it leads to the understanding of the complexity of the control system and more fundamentally leads to clinical implications. If Listing's law is implemented by the eye muscles, an abnormality in eye orientation can be corrected for by repairing the eye muscles. Under certain conditions it has been shown that Listing's law can be violated suggesting a neural implementation. For example, during sleep Listing's law is transiently violated (Nakayama, 1975). Moreover, Listing's law is violated during vestibuloocular slow phase eye movements that rotate the eye opposite to the head during head movements such as to keep the axis of rotation of the eye collinear with the head (Crawford and Vilis, 1991). Other studies have also focused on the positioning of Listing's plane itself as evidence for neural implementation. For example, during vergence (when the two eyes rotate nasally) the Listing's planes for the two eyes rotate outward resulting in new torsional values of the eyes for any single gaze direction (Mok et al, 1992). This and further studies have led to the general conclusion that Listing's law is neurally implemented.

Donders'law of the head and the Fick-gimbal strategy. The head motor system was initially ignored since earlier studies (Bizzi et al, 1971) concluded that during gaze shifts movements of the head were insignificant and did not contribute to the overall shifting of the line of sight (Goossens and Van Opstal, 1997). Subsequent studies, albeit controversial, found this to be untrue (Guitton and Volle, 1987; Tomlinson and Bahra, 1986; Tabak et al, 1996) and further research on the similarity and differences between the oculomotor system and the head motor system came into fruition.

The head, as discussed, is capable of rotating in all three dimensions similar to the eye. One would thus presume that the head would behave like the eye in that it would be constrained by the same laws, i.e. Donders' law, and use a similar strategy to implement Donders' law, namely Listing's law. Initially it was observed that final head positions fall into a 2-D plane indicative of Listing's plane, suggesting that the head motor system adopts a strategy similar to the eye in order to obey Donders' law (Straumann et al, 1991; Tweed and Vilis, 1992). However the range of head movements examined in one of these studies, Straumann and colleagues (1991), was relatively small (±25°) and did not accurately reflect the large amplitude of head movements that are normally made during natural gaze shifts. Glenn and Vilis (1992) examined a larger range of head movements more representative of natural head movements. They reported that the head did not follow a Listing's law strategy since 3-D head orientation vectors did not fall into a flat plane, rather they were restricted to a twisted, bow-tie like surface (figure 4C). Thus it appeared that for these movements, the horizontal and vertical axes of rotation were not independent of each other (for Listing's law to be true they must be independent). Moreover, the final positions reached by the head were similar to those that would occur if head position was being assigned in Fick coordinates, i.e. the head first rotates about a body-fixed vertical axis, then about a head-fixed horizontal axis, and finally a head-fixed torsional axis. In this system, vertical position of the head is dependent on the amount of horizontal rotation, and torsional position is dependent upon both the horizontal and vertical positions of the head. Although the strategy is different, Donders' law is still upheld through the implementation of the Fick strategy by virtue of assigning a zero torsional value in Fick coordinates.

Figure 4 graphically represents the implementation of the Fick strategy. Part A plots model simulated final head orientations (as in figure 3) that would be adopted if the head obeyed the Fick strategy (A) and the corresponding orientation vectors (plotted as quaternions) as viewed from the front (B) and the side (C) of the subject. The same convention is used as in figure 3. In part A, the nesting of the axes can be observed by the shortening of the horizontal axis (i.e. the bar that runs through the ear) in final head orientations 1, 2, 4, 5, 6, and 8. The shortening of the bar reflects the tilting of the axis away from the plane of the paper, which in turn represents the change in position of the horizontal axis when there is horizontal rotation about the vertical axis. When we examine these same orientation vectors from the side of the subject in coil coordinates, the orientation vectors tilt away from the vertical axis and have a torsional component. These vectors form a bow-tie like pattern indicative of the nested axes of a Fick-gimbal. Since orientation vectors 2, 4, 6, 8, have a torsional component, then the corresponding final head orientations (A) should have a counterclockwise (CCW) or clockwise (CW) tilt. When these final head orientations are examined in A, compared to their counterparts in figure 3A, these head orientations do have a torsional tilt in either direction.

Figure 4

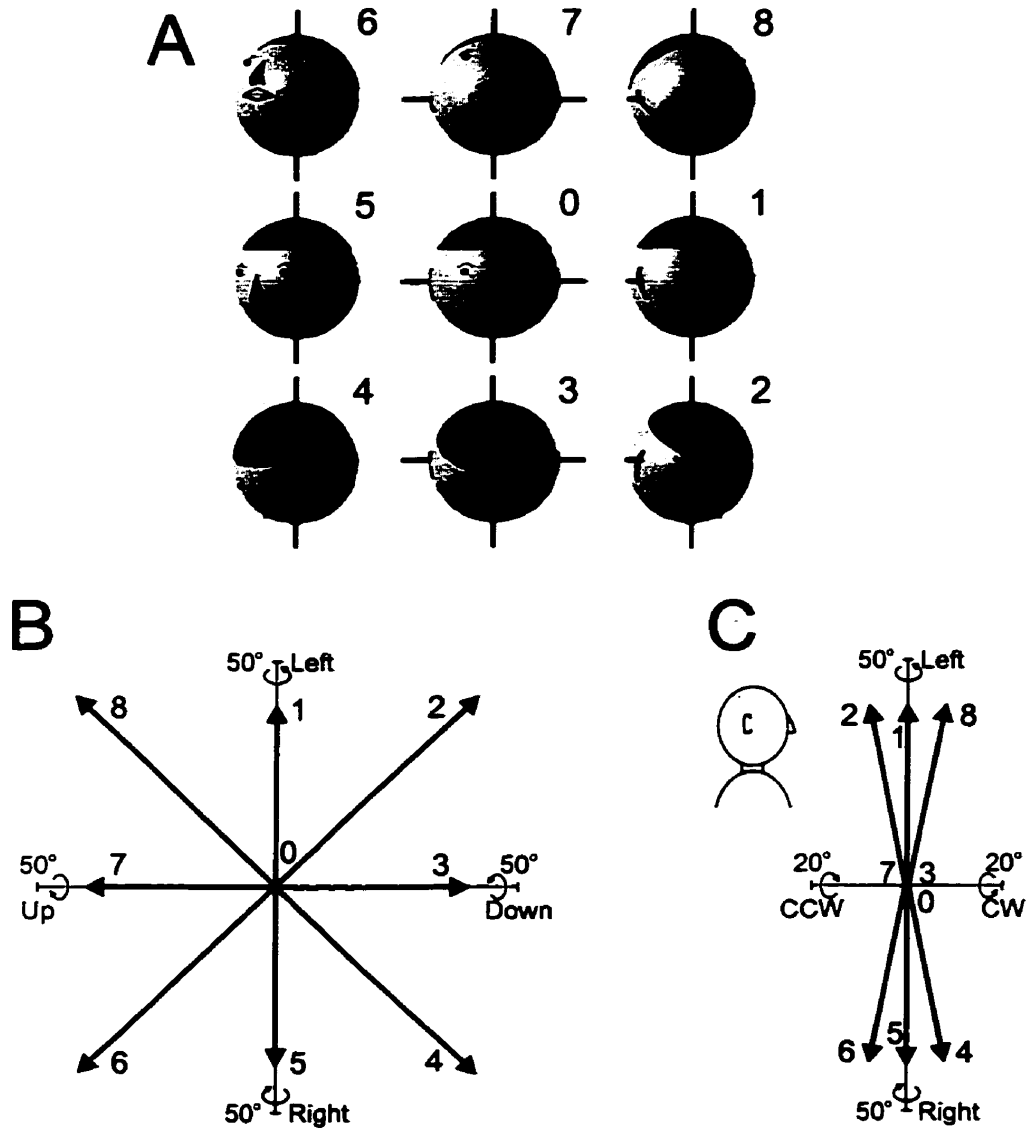

Figure 4. Hypothetical kinematics of a head obeying Fick-gimbal strategy. ***A***: hypothetical final head positions assumed by rotation from center to each of the 8 targets (same convention as in figure 3). ***B***: frontal (i.e. horizontal vs. vertical axes) projection of the distribution of head orientation vectors for final head positions in A plotted in space-fixed coordinates. Vectors are plotted as quaternions such that the right-handed rule applies. Orientation vectors are labeled with their corresponding number, e.g. 1 in B is the orientation vector for final head position 1 in A. ***C***: same distribution of orientation vectors in B but viewed from the side (i.e. vertical vs. torsional axes). The space-fixed distribution of orientation vectors form a bow-tie like pattern, similar to previous studies (Glenn and Vilis, 1992; Radau et al, 1994).

Perceptual and functional consequences of Donders' Law. Why would the gaze motor control system choose to constrain eye movements via Listing's law, and the head via the Fick-gimbal strategy? Several hypotheses on the perceptual consequences of both strategies have been proposed. For Listing's law, the first proposal is that it optimizes the perception of radial lines on the retina (Hering, 1868) such that radial constancy is maintained throughout the gaze shift. The second proposal is that Listing's law optimizes binocular vision by maintaining a constant positional relationship between the two eyes (Crawford and Vilis, 1991). The third is that Listing's law optimizes the path of saccades to and from center by choosing the shortest possible path (Tweed and Vilis, 1990). Finally the fourth possibility is that by maintaining the extraocular muscles at the center of their torsional range of motion, the workload is minimized (Fick, 1854; Wundt, 1859; Nakayama, 1983; Tweed and Vilis, 1990; Radau et al, 1994).

The perceptual and functional consequences of the Fick-gimbal strategy are different from those of Listing's. The Fick strategy could choose to optimize the perception of lines on the horizon by keeping the head (a line through the two eyes) parallel with the horizon (Glenn and Vilis, 1992; Hore et al, 1992; Klier and Crawford, 1998). The second possible purpose of the Fick strategy would be to optimize for binocular vision by aligning the two eyes with the horizon (Crawford and Vilis, 1995). The third possible advantage of the Fick strategy would be to optimize for perceived tilt in visual and/or vestibular stimuli such that by keeping the head upright and parallel to the horizon, object perception is optimized (Rock et al, 1981; Crawford and Vilis, 1995; Crawford et al, 1999).

The fourth possibility is that the Fick strategy may work to minimize the workload on the neck muscles by allowing the head to move more horizontally and the eyes to move more vertically to redirect gaze such that work done against gravity is minimized (Glenn and Vilis, 1992; Radau et al, 1994). This seems to be a plausible explanation since studies performed with animals and humans have shown that the head contributes more to the horizontal component of gaze and the eyes to the vertical component of gaze (Glenn and Vilis, 1992; Crawford and Guitton, 1997; Freedman and Sparks, 1997). Likewise, the Fick strategy may optimize for the motion of the cervical vertebrae since the first and second cervical vertebrae (atlas and axis, respectively) are anatomically similar to a Fick-gimbal system with the atlas behaving like the horizontal axis and the axis vertebra behaving like the vertical axis (Richmond and Vidal, 1988; Glenn and Vilis, 1992; Radau et al, 1994).

Finally, it has been proposed that the Fick-strategy may be best suited for ease of coordination with the arm and the eye (Straumann et al, 1991; Theeuwen et al, 1993). By by coordinating the eye, head, and arm through a common constraint, i.e. Donders' law, Bernstein's principle of motor synergies is upheld. According to Bernstein's concepts, the brain attempts to apply the smallest number of control parameters at each level of the motor system (Straumann et al, 1991), thereby eliminating redundant degrees of freedom (Bernstein, 1967).

However up until now it has not yet been established which of these arguments are valid in determining what strategy best upholds Donders' law in its attempt to eliminate kinematic redundancy in the gaze motor control system.

One possible method in discerning between these arguments for the head motor system has been used by Crawford and Guitton (1997) and Misslisch and colleagues (1998). The method involves reducing the effective visual range by having subjects wear opaque goggles with an aperture over the right eye. Crawford and Guitton (1997) and Crawford and colleagues (1999) reported that in monkeys, gaze shifts made with pin-hole goggles (restricted vision to ± 4°) produced remarkably different behaviors relative to natural gaze shifts without the goggles. For instance, when the monkey made random gaze shifts, the pattern of head movement changed in several ways: the amplitude of head movement increased; the head contributed more to vertical movement than normal; distribution of head orientation vectors was altered from the normal Fick-like twist to a flattened, almost Listing's type distribution. This was a surprise finding since an earlier study (Theeuwen et al, 1993) reported that when head amplitude increased, by having subjects point their nose at the targets, the Fick-like twist of the plane of head orientations became even more twisted, not flattened. The finding that the distribution of head orientations are different when the size of head movements is increased for monkeys and humans raises the question of whether humans and monkeys utilize different strategies in coping with task constraints. Our main goal for this study, therefore, was to determine if humans would replicate the results with pin-hole goggles as observed in monkeys

(Crawford and Guitton, 1997), if so why this occurs, and what perceptual consequences are being optimized in the choice of strategies taken by the head and gaze motor systems.

Determining the constraints optimized for head posture. The results of this study will show that by employing the pinhole goggles task in humans, the form of Donders' law for the head will be altered in a manner to accommodate the reduced visual range, confirming that the choice of strategies is neurally imposed. By imposing different constraints through variations of the goggles task it will be determined which of the factors (binocular vision, peripheral vision, range of head motion, or motor demands on the head) are optimized in determining which strategy is chosen in shaping head posture.

METHODS

A total of ten subjects (6 female, 4 male; ranging in age from 23 to 44 without known eye or head movement disorders) participated in our study with seven of those also completing a second, third and fourth experiment. The study was pre-approved by the York University Human Participants Review Subcommittee and informed consent forms were signed by each of the participants before each of the experiments.

Three-dimensional head orientations were measured using the 3-D magnetic search coil technique, as described elsewhere (Tweed et al, 1990; Glenn and Vilis, 1992). Head positions, unless stated otherwise below, were measured using a homemade, 3-D coil adhered to a snugly fit swim cap. In addition, right eye positions were measured in the first subject during our preliminary experiments using a 3-D scleral (Skalar) search coil in order to ascertain whether eye movements affect the overall behavior of the head. Subjects sat in a lighted room with their torso fixed in an earth-fixed chair in the middle of three mutually perpendicular magnetic fields (frequencies of 90, 124, 250 Hz) which were generated by 2 m in diameter field coils. The three voltages from each coil were sampled at 100 Hz. Calibration procedure and accuracy was similar to those described previously (Henriques et al, 1998; Klier and Crawford, 1998). Translational positions of the head were not measured.

Target arrays. Subjects were required to make eye-head gaze shifts between white dots (10 mm diameter) on a black tangent screen located 1.1 m from the subject's right eye. The standard range (figure 5) consisted of 9 targets (white dots) arranged in a square grid centered in front of the right eye. The 4 cardinal targets (i.e. targets on the vertical and horizontal axes) were placed 40° from the central target (intersection of the horizontal meridian and the midsagittal plane) with the 4 oblique targets placed 48° from center, in the corners. Experiment 2 through 4 had an additional reduced range paradigm (figure 5), resembling a rectangular box, with the following dimensions: 2 25° horizontal targets (left and right of center); 2 20° vertical targets (above and below center); and 4 28° oblique targets (placed at the 4 corners). These dimensions were selected to represent the normal range of head movements observed when a subject made unrestricted gaze shifts to targets of the standard range. Subjects were initially asked to fixate the center target at the beginning of every paradigm for use as a reference position. Participants were then verbally instructed to redirect their gaze to fixate targets, with a between targets time interval of approximately 2 seconds. For example, the experimenter would call out up-left, down-right, middle-center, etc. as in a previous gaze control experiment (Glenn and Vilis, 1992). Each block consisted of a trial for each of the nine targets, with every paradigm consisting of 5 blocks (duration of paradigm: 100s period). The range of targets was chosen such as to obtain an even range and distribution of final positions for quantifying Donders' law.

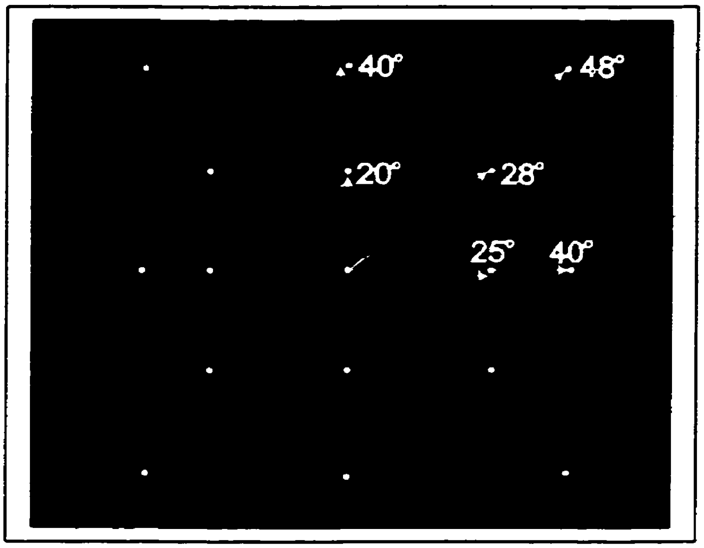

Figure 5. A visual schematic of the target locations. The standard range: 4 40° cardinal targets and 4 48° oblique (i.e. corner) targets; and reduced range: 2 20° vertical targets, 2 25° horizontal targets, 4 28° oblique targets.

Tasks. The purpose of experiment 1 was to describe the effect of reducing the useful oculomotor range on 3-D head orientation range. Subjects performed 2 paradigms: control and standard goggles. The first paradigm involved subjects making head-free gaze shifts to the targets of the standard range. For the second paradigm, subjects wore goggles that completely occluded vision except for an aperture (5 mm in diameter) that reduced the headcentric visual range to 10°. The location of the aperture was first selected as the median of eye positions (across 5 subjects) used to gaze straight ahead (without goggles). Subjects made head-free gaze shifts to the targets of the standard range with these goggles on. Those subjects who demonstrated a statistically significant change in head posture (i.e. decrease in the a_5 score, formula 2) continued testing to determine the factors that contributed to this change.

Experiment 2 attempted to delineate what task constraints determined head posture: binocular vision, peripheral vision, amplitude of head movement, or motor coordination. Seven subjects were exposed to 5 different paradigms in the following order: (1) control; (2) monocular paradigm; subjects wore a left eye patch; (3) standard goggles paradigm; (4) binocular goggles paradigm; subjects wore the pin-hole goggles with apertures in the center of each of the two visual fields; (5) reduced head range paradigm; subjects made gaze shifts with the standard goggles to the reduced range.

The purpose of experiment 3 was to differentiate between the effects of peripheral vision and motor coordination on 3-D head range. This experiment required the same 7 subjects from the previous experiment to perform various tasks. For the first half of the experiment, subjects wore a helmet with a laser pointer attached on top via a universal joint positioner (the weight of the full helmet apparatus was 380 grams). A 3-D coil was adhered to the helmet, which was fastened to the subject's head with chin-straps and made to fit tightly by having subjects wear a cap. Prior to testing, subjects were asked to fixate the center target with the helmet and goggles on. The laser pointer was then adjusted to point at the center target as viewed by the subject with the goggles on. The goggles were then removed. The first paradigm was the control helmet condition in which subjects made unencumbered gaze shifts to the targets of the standard range (i.e.

laser off). The second and third paradigms required subjects to land the laser on targets of the standard and reduced ranges respectively. The second half of the experiment required subjects to remove the helmet and don the swim cap and standard goggles. Subjects were then instructed to repeat the control and goggle paradigms of the previous experiment (to standard range) for comparison.

The purpose of experiment 4 was to determine if the head motor control system optimizes Donders' law specifically for redirecting gaze. This experiment was similar to experiment 3 with the same 7 subjects. Subjects were first asked to repeat a control helmet condition similar to that of experiment 3. Subjects were then instructed to land the laser on targets of the reduced range. The final paradigm involved subjects fixing their gaze on the center target while they only moved the laser (i.e. their head) to targets of the reduced range. Thus in the final paradigm the subject's gaze was fixed on the center target and only the head was permitted to move.

Data Analysis. The coil signals from the eye coil and head coil were sampled at 100 Hz and recorded on-line by a personal computer. Reference positions of the right eye and head were made by having subjects look straight ahead at the center target at the start of the control conditions. These signals were then used to compute quaternions (Tweed et al, 1990) to represent orientations of the eye-in-space (Es) and head-in-space (Hs), defined by the angle and axis of rotation from the reference position (Tweed et al, 1990; Tweed et al, 1995). These quaternions, Es and Hs, are expressed in a right-handed coordinate system that is aligned with the coils. Eye-in-head (Eh) was computed from Es and Hs as described previously (Tweed et al, 1990).

Quaternions are represented as the sum of a scalar (q_o) and a vector (q)

$$q = q_o + \boldsymbol{q} = \cos(\alpha/2) + \sin(\alpha/2)\mathbf{n} \tag{1}$$

where α is the angle of rotation from a reference position and **n** is the unit vector lying along the axis of rotation is **n** (Tweed et al, 1990). Since quaternions are expressed in right-handed coordinates, by aligning one's thumb along **n** (the axis of rotation), pointing it in the same direction as the vector, the curling of the fingers will describe the rotation. For example for up-ward rotations, the thumb would point rightwards and the fingers would curl in the up-ward direction. The length of the vector lying along the axis of rotation is defined by $\sin(\alpha/2)$ and **n** has three orthogonal components: q_1 represents the torsional component; q_2 the vertical component; q_3 the horizontal component.

Two dimensional (2-D) gaze direction or head facing vectors were then computed from quaternions (Tweed et al, 1990). For purpose of display, these unit vectors were projected onto a frontal plane aligned with the horizontal and vertical magnetic fields.

To quantify the 3-D pattern of head orientations in each task, the amount of twist in the H_s surface was computed by fitting a second-order surface of best fit to the H_s quaternions (Tweed et al, 1990; Tweed and Vilis, 1990; Glenn and Vilis, 1992; Radau et al, 1994; Medendorp et al, 1998; Misslisch et al, 1998; Crawford et al, 1999). Only points where the head velocity was < 10°/s were selected. A second-order fit is described by the following equation, which expresses torsional position (q_1) as a function of vertical (q_2) and horizontal position (q_3):

$$q_1 = a_1 + a_2q_2 + a_3q_3 + a_4(q_2)^2 + a_52q_2q_3 + a_6(q_3)^2 \quad (2)$$

The fifth term (i.e. a_5) describes the "twist score" which quantifies the amount and direction of a twist in a given surface. In general the higher the a_5 score, the greater the amount of twist in the surface (in either the positive or negative direction). For example, for a surface that is planar, e.g. for Listing's plane, the a_5 score would generally be close to or equal to zero.

From the 2-D surface of best fit, standard deviations, termed torsional thickness, were also computed to quantify how closely the head orientations cluster around their H_s surface in the direction of q_1 (Tweed et al, 1990; Glenn and Vilis, 1992; Crawford et al, 1999). In general, the smaller the torsional thickness score, the closer the H_s quaternions stay to their surface and therefore the better they conform to Donders' law.

For a simpler and more meaningful measure of the twist in the *Hs* range, gimbal scores were calculated (Glenn and Vilis, 1992; Crawford ët al, 1999) by the following equation that describes gimbal systems

$$q_1 = s(q_2q_3/q_0) \quad (3)$$

The gimbal score (s coefficient) allows for better comparison in surface shapes along a continuum ranging from the twisted bow-tie generated by Fick gimbals, s coefficient of –1, through the plane produced by a system that follows Listing's law, s coefficient of 0, to the oppositely twisted bow-tie generated by Helmholtz gimbals, s coefficient of +1. This value is reported in the figures as the gimbal score. Statistical analysis was performed with the SPSS Statistical Package and consisted of two-tailed paired sample t-tests unless otherwise specified.

RESULTS

General Observations: eye-head coordination. The pin-hole goggles technique has been used before in primates (Crawford and Guitton, 1997; Crawford et al, 1999) and in humans (Misslisch et al, 1998) as a means of demonstrating the plasticity of the gaze motor control system. In this study, therefore, this task and its consequence on the overall gaze motor control system was initially examined. Figure 6 shows one way that the pin-hole goggles alter the coordination of the eye and head. It depicts final two-dimensional gaze direction during fixation as viewed from behind subject 1 (as indicated by the head caricature). The top row illustrates random gaze shifts (Es) to the nine targets: center target, 4 targets at 40° retinal displacement along the cardinal axes (horizontal and vertical), and 4 targets at 48° retinal displacement in the oblique directions (4 corners) during control (A) and (D) goggles tasks. It can be seen in this figure that the subject is able to acquire all nine targets in both conditions (A/D). The difference between the two tasks becomes apparent only when 2-D gaze is decomposed into its relative components, Eh (second row) and Hs (last row). In the control task (B), Eh contributes mostly to vertical gaze as most previous studies have found (Glenn and Vilis, 1992; Crawford and Guitton, 1997; Freedman et al, 1997). In contrast, in the goggles task (E), final Eh position was relatively confined to the headcentric 10° visible range provided by the aperture (denoted by the ring in E).

Figure 6

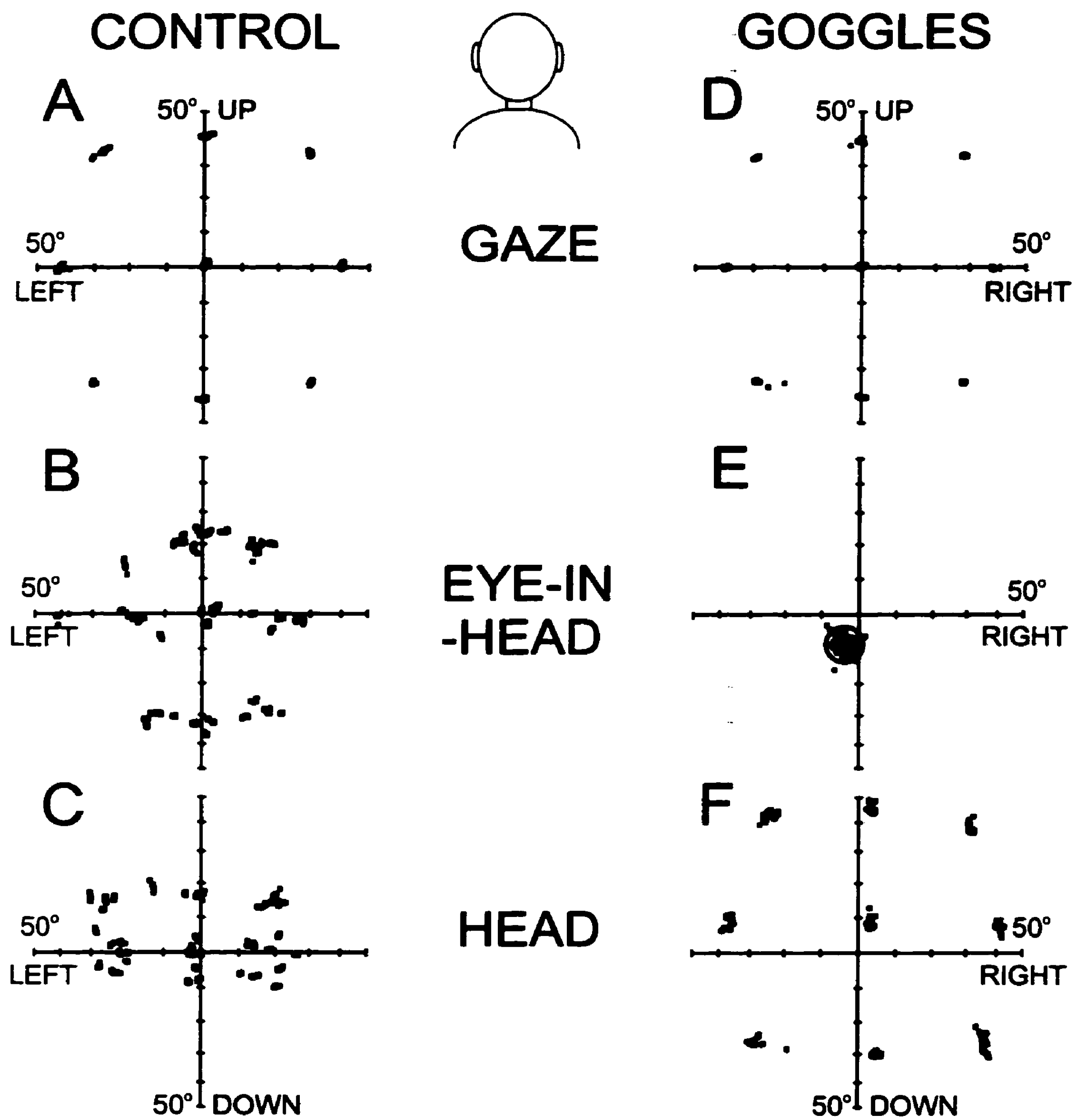

Figure 6. Frontal projections of two-dimensional pointing vectors: distribution of gaze, eye, and head fixations during control (*A-C*) and standard goggle (*D-F*) conditions as viewed from behind one subject during head-free gaze shifts to the 9 targets. Data points were selected as final fixation points where eye, head, and gaze were < 10°/s. Cardinal targets were placed at 40° eccentricity and the oblique targets at 48°. Goggles restricted the effective visual range to approximately 10° (denoted by the ring in *E*). Top row: gaze. Middle row: eye-in-head. Bottom row: head-in-space. -

Examination of final 2-D head positions (C and F) reveal an analogous difference between the control and goggles tasks. In the control condition (C), the *Hs* component contributes mostly to horizontal gaze (Glenn and Vilis, 1992; Freedman et al, 1997). However, due to the decrease in the contribution of *Eh* to overall gaze in the goggles condition and the observation that gaze acquires the target accurately; there should be an associated increase in *Hs* contribution. In (F), the subject increases *Hs* contribution to the extent that *Hs* becomes the primary mover of gaze. Thus, as shown previously in monkeys and humans (Crawford and Guitton, 1997; Misslisch et al, 1997), subjects were able to acquire all targets accurately by consistently driving the eye to the location of the aperture and concomitantly increasing the amplitude of the head movement, such that the final *Hs* positions essentially equal final *Es*. How were subjects able to accomplish this? Two possibilities: (1) zero eye movement; or (2) normal eye movement with a big VOR response.

Figure 7 plots four amplitude vs. time traces of vertical gaze shifts from 40° down to 40° up (largest possible target range). The top panel represents *Es*, *Hs*, and *Eh* traces made during the control condition (no goggles), while the bottom panel illustrates those traces made during the standard goggles condition. As was depicted in figure 4, *Hs* vertical amplitude is smaller than the amplitude of *Eh* in the control condition. In contrast during the goggles condition, (B), *Eh* is relatively confined to the aperture consequently resulting in an increase in the amplitude, and hence contribution, of *Hs*. Although Hs became the primary contributor of gaze, saccades still occurred. The

Figure 7

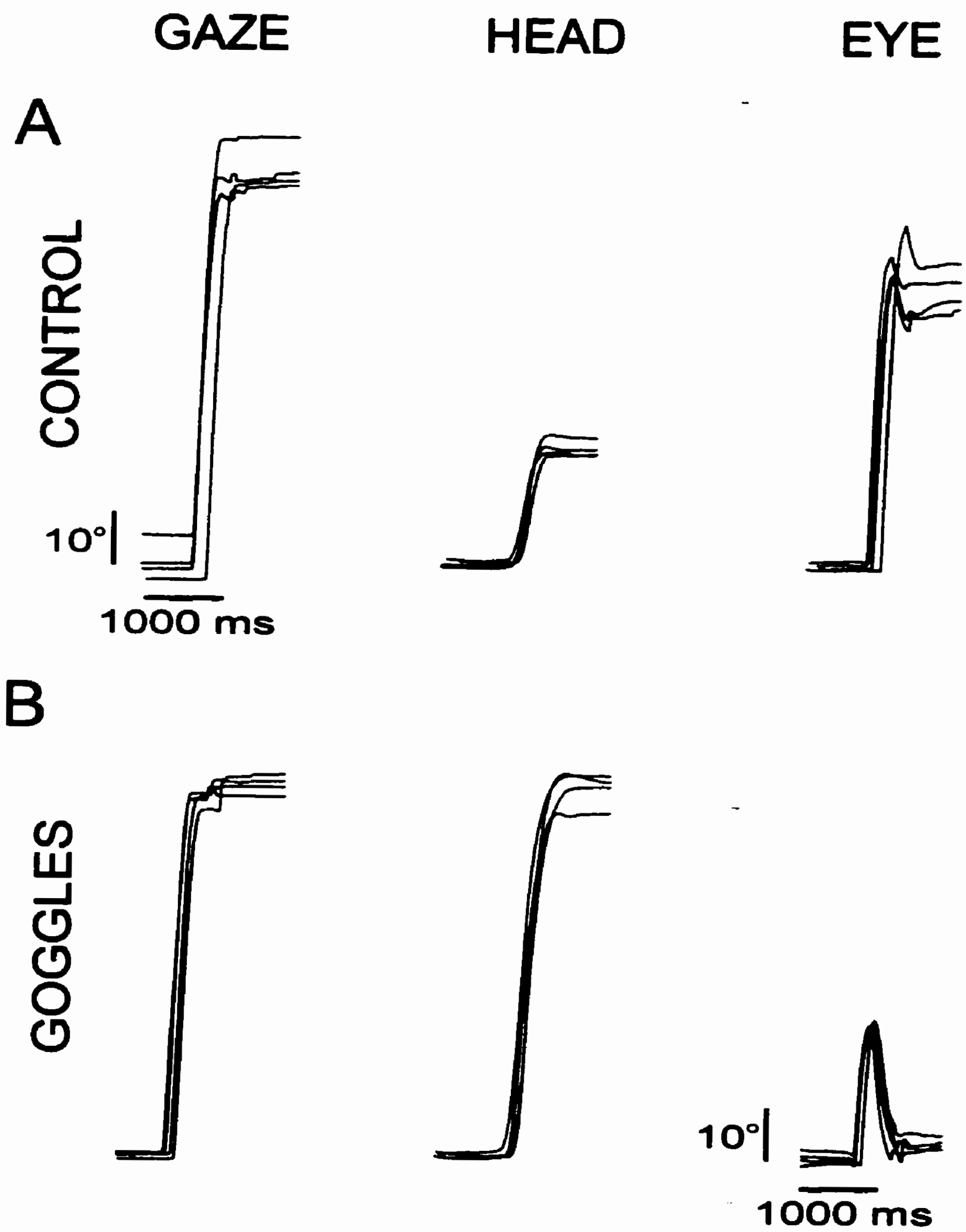

Figure 7. Temporal kinematics of gaze, head, and eye for vertical movements during control (*A*) and standard goggle (*B*) conditions. Trajectories reflect four 80° movement from a 40° down target to 40° up target during a 2 s interval.

saccade amplitude decreased but did not disappear, and the VOR subsequently returned the eye to the aperture. These observations agree with previous descriptions (Crawford and Guitton, 1997; Misslisch et al, 1998; Crawford et al, 1999) and will not be further quantified here.

Does the goggle paradigm affect Donders' law of the head in humans? Based on the finding that in monkeys the shape of the associated 3-D head range surface significantly changes with task demands (Crawford et al, 1999), the first task was to examine the 3-D human head range during the goggles paradigm to investigate whether Donders' law was still adhered to, and if it was altered in any way. Figure 8 plots three head trajectories (large squares) between each of the four oblique targets for purely horizontal and vertical movements during the control (top row) and goggle (bottom row) paradigms viewed from the front (A and C) and the side (B and D) of one subject. The trajectories are represented as quaternions so the right-handed rule applies (see methods). The squares represent the tip of a virtual vector emanating from center, with the length of the vector corresponding to the magnitude of rotation.

In the control condition (A), head movements used to redirect gaze to the four targets is much more variable in comparison to the movements observed in the goggle condition (C) despite the accuracy of gaze (also plotted in A as smaller squares for comparison). In the side view for the control condition (B), these same trajectories form the classic Fick-like twist similar to the twisted distribution of orientation vectors

Figure 8

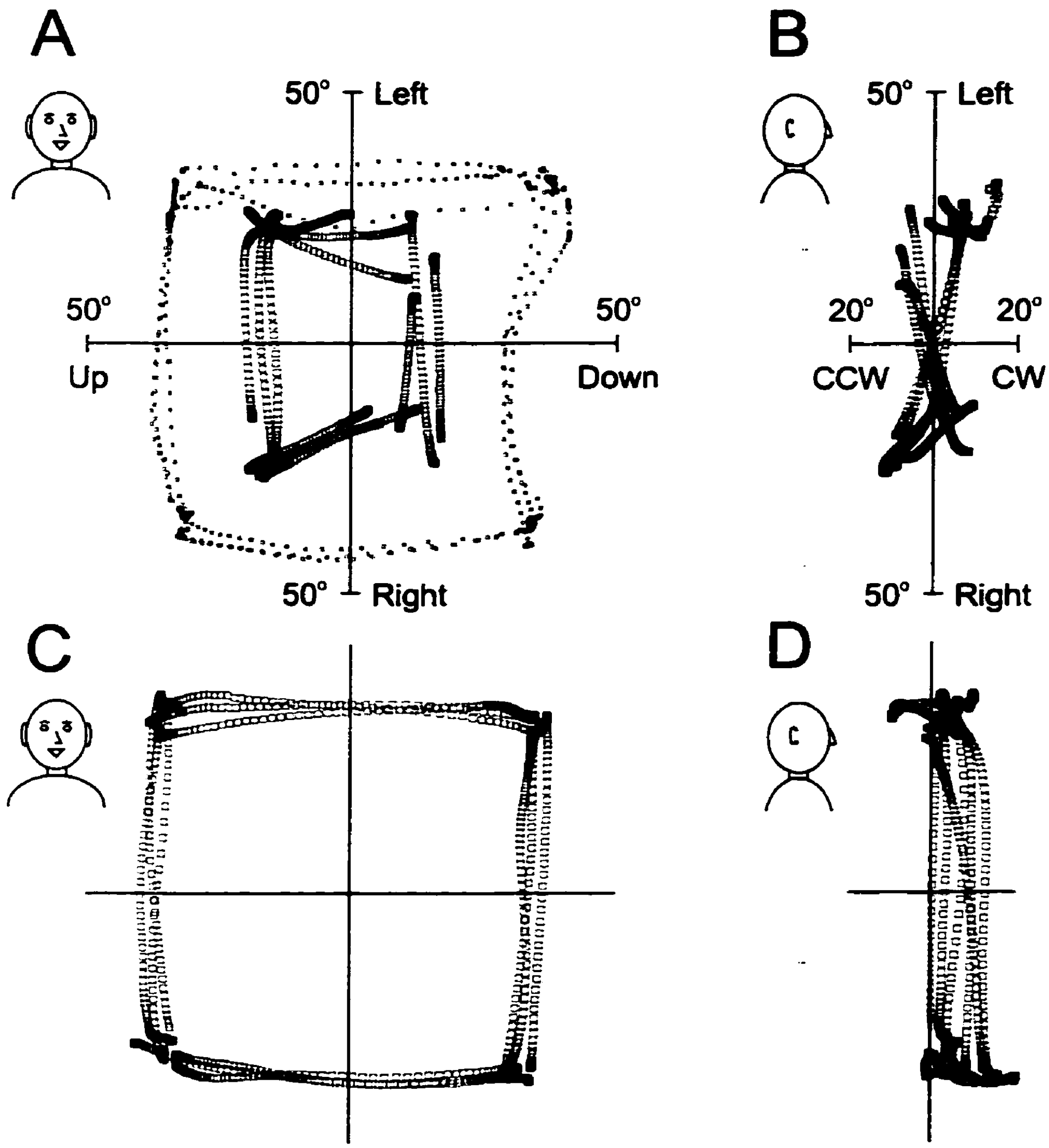

Figure 8. Three-dimensional head-in-space kinematics during movements in the control (*A* and *B*) and goggle (*C* and *D*) conditions. Data was selected based on 3 purely horizontal or vertical movements to each of the four oblique targets placed at 48°. *A and C*: 2-D kinematics of head-in-space (large squares) and eye-in-space (small squares, only in *A*) orientations viewed as frontal projection (head/shoulder caricature indicates space-fixed ordinates) of quaternions during control (*A*) and goggle (*C*) conditions, using the right-handed rule (horizontal axis flipped due to frontal view). Second column (*B and D*): 3-D kinematics of head-in-space orientations showing side projection of quaternion vectors, i.e. horizontal position as a function of torsion during the control (*B*) and goggle (*D*) conditions.

illustrated in figure 4C. The range, as expected, increased in the goggles condition (C) relative to the control condition (A). In the side view for the goggle condition (D) the trajectories are less twisted in comparison to the control (C) and seemed relatively more similar to the flat plane of orientation vectors observed in figure 3C. The finding that the trajectories become less twisted with increased range is unexpected because previous studies have suggested that increasing target eccentricity, or head range, would produce more fanning and subsequently greater twisting (Glenn and Vilis, 1992).

Subjects also made oblique movements to these same targets (e.g. movement from lower right target to upper left target). It was observed that during oblique movements, the trajectories transiently violated the Fick constraint, as observed in monkeys (Crawford et al, 1999), only returning the head to the Fick range at the end of movements. For this reason, only head fixation points (where the head was moving at < 10 °/s) were considered for the remainder of the analyses.

Figure 9 (A and B) plots these fixation points for one subject as quaternion vectors, with the points representing the tip of a virtual vector emanating from center (reference point), and the length of this vector corresponding to the magnitude of the rotation (plotted from the side perspective). In accordance with figure 6 (C and F), the 2-D range of final head positions in the goggles condition (B) was larger compared to the control condition (A). Despite this, the torsional range appears to be smaller. However, from these two head fixation point plots it is difficult to determine whether there is a difference in the surface shapes or a change in torsional variance.

Figure 9

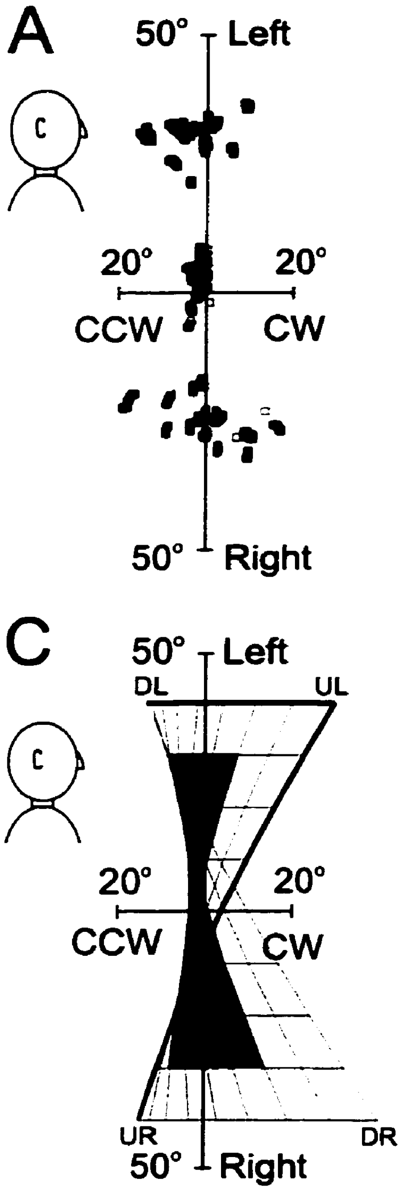

Figure 9. Comparison of 3-D head orientation ranges during fixation of the 9 targets in the control (*A* and *C*) and goggle conditions (*B* and *D*) of experiment 1. ***A and B***: quaternion vectors plotted from the side perspective using the right-handed rule for subject S.P during control (*A*) and goggle (*B*) conditions. Only fixation points were considered, i.e. where head speed was < 10°/s. ***C and D***: 2nd-order surface fits to the fixation data in *A* and *B*. Each grid indicates 10° horizontal/vertical across the surface, with a 40° X 40° limit (extent of the range of data for the goggle condition). The shaded area reflects the actual data range (i.e. data range of *A* and *B*). Thickened lines correspond to the upper and leftward edges of the fit (DL, down-left; UL, up-left; DR, down-right; DL, down-left) according to gaze direction.

To clarify this, a 2nd order surface was fit to these fixation points, as done in previous similar studies (Glenn and Vilis, 1992; Theeuwen et al, 1993; Radau et al, 1994; Medendorp et al, 1998; Misslisch et al, 1998; Crawford et al, 1999). Figures 9C and D are examples of 2-D surfaces of best fit to the data range illustrated in (A) and (B), where each grid denotes 10°. The darkened portions of (C) and (D) represent the actual data range in (A) and (B). However, to standardize across all tasks, only surfaces of best fit over a constant 40° X 40° range are shown, corresponding to the largest head range obtained in the goggles paradigm. The rationale for standardizing the surface fit illustrations was to minimize any visual misconception of the shape of the surface fit and the corresponding gimbal score, while still showing the actual data range (gray portion).

The amount and direction of twist observed in the control (fig. 9C) is indicative of a Fick-gimbal system, as reflected by the characteristic twist in the thickened leading edge. Relative to our space-fixed orthogonal coordinates, *Hs* assume a counterclockwise orientation in the down-left (DL) and upright positions (UR); and a clockwise orientation in the up-left (UL) and downright (DR) positions in orthogonal space coordinates. Figure 9D represents a 2-D surface fitted to the goggles data range of (B). In contrast to the strong Fick-like shape of the surface representing the control range (C), the surface was somewhat flattened with a lesser twist in the goggles condition (D), possibly signifying a task-dependent modification of the head Fick strategy.

To quantify the amount of twist in the two conditions, the average gimbal score was calculated (across subjects) for *Hs* for the control and goggles paradigms. Figure

10A shows the average gimbal score (and SE) for 10 subjects across all paradigms (as presented to the subject in order, with each paradigm being 100s in duration) with the hatched bars representing the control and the white representing the goggles condition. On average compared to controls, there was a significant overall decrease of 56% in the gimbal score of the head range as a result of the goggle task (across subjects ($p \leq .021$), reflecting a general flattening of the surface. This suggests a similar task-dependent effect to that reported in monkeys (Crawford and Guitton, 1997; Crawford et al, 1999).

Quantifying the surface twist as a gimbal score provides a means of measuring the twist in the surface final *Hs* orientations but does not provide information about whether these final head positions adhere to the surface in a systematic manner, i.e. how well they obeyed Donders' law. The lower panel (B) of figure 10 illustrates the overall average of the torsional thickness score (in degrees) of *Hs* position during the control tasks (striped) and the goggles tasks (white). The torsional thickness score is highly consistent and on average 1.622° for the control condition. On the other hand, the overall torsional thickness of the goggles task increased by 37% to 2.222°, statistically significant ($p \leq .01$) as indicated by the asterisk.

However, up until this point 2-D horizontal and vertical ranges were not controlled for. In particular, the latter increased on average 56% and the former 36%, respectively. Therefore, it was unclear whether the slight increase in torsional thickness was due to a range effect or a fundamental degradation in Donders' Law. Similarly, it was not yet clear if the range "flattening effect" was due to such degradation, or to some

Figure 10

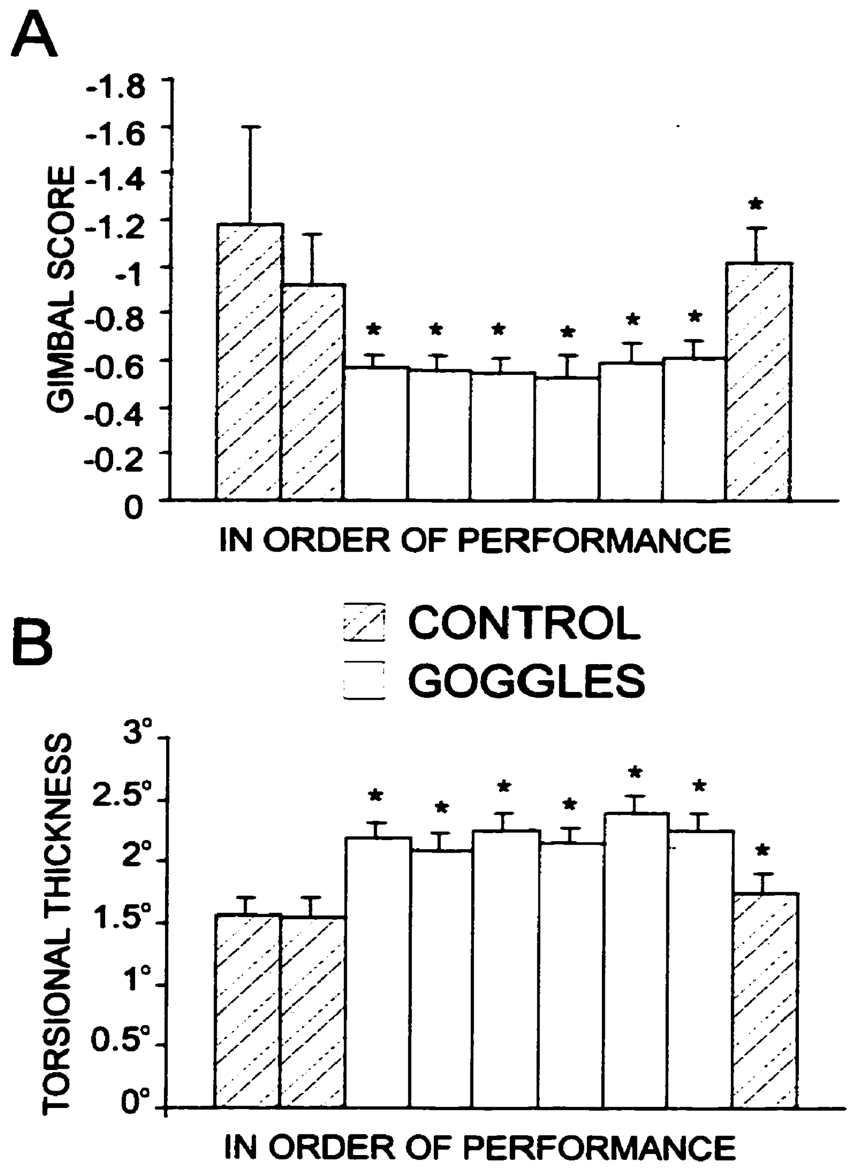

Figure 10. Quantitative comparison of the gimbal and torsional thickness scores for head orientation ranges of experiment 1. ***A***: quantitative comparison of the gimbal score (see methods). Each bar represents the average gimbal score across all 10 subjects and standard error for each paradigm presented in order of performance (100s intervals). ***B***: quantitative comparison of the torsional thickness score of the head orientation range to the fitted surface. Each bar represents the average torsional thickness score, in degrees, and standard error across all 10 subjects for each paradigm presented in order of performance. * indicates significance ($p < .05$, two-tailed) relative to the control condition.

as yet unspecified task constraint. Answering these questions was the purpose of our next experiment.

Task-dependency. Several hypotheses as to why the flattening of the head range surface transpires have been formulated. These hypotheses include: the loss of input from one eye due to the goggles, suggesting a binocular role in head movement; loss of peripheral vision due to goggles, suggesting an alignment of the head with the structure of the room; and a mechanical effect, a byproduct of an increase in head range or a degradation in Donders' law. Of the ten subjects who participated in the first experiment, seven demonstrated a significant decrease in the twist score as a result of the goggles paradigm. Consequently, these seven subjects participated in a second experiment.

Figure 11 illustrates the results of the various tasks (control, left-eye patch, dark, standard goggles, binocular goggles, reduced range) that were employed to test each of these hypotheses. Part (A) represents the 2-D surfaces of best fit, as viewed from the side, for one representative subject to each of these paradigms, presented in a logical order. The conventions used are the same as for figure 4, i.e. 40° X 40° fit illustrated with actual range shaded. The remainder of the figure shows gimbal fits (B) and torsional thickness scores (C) averaged across subjects, in order of performance.

The surface fit for the control condition was, as expected, a Fick-gimbal like twist similar to that observed in experiment 1 (figure 9C). In addition, the surface fit for the goggles condition (figure 11A, goggles) yielded a surface similar to the result obtained in

Figure 11

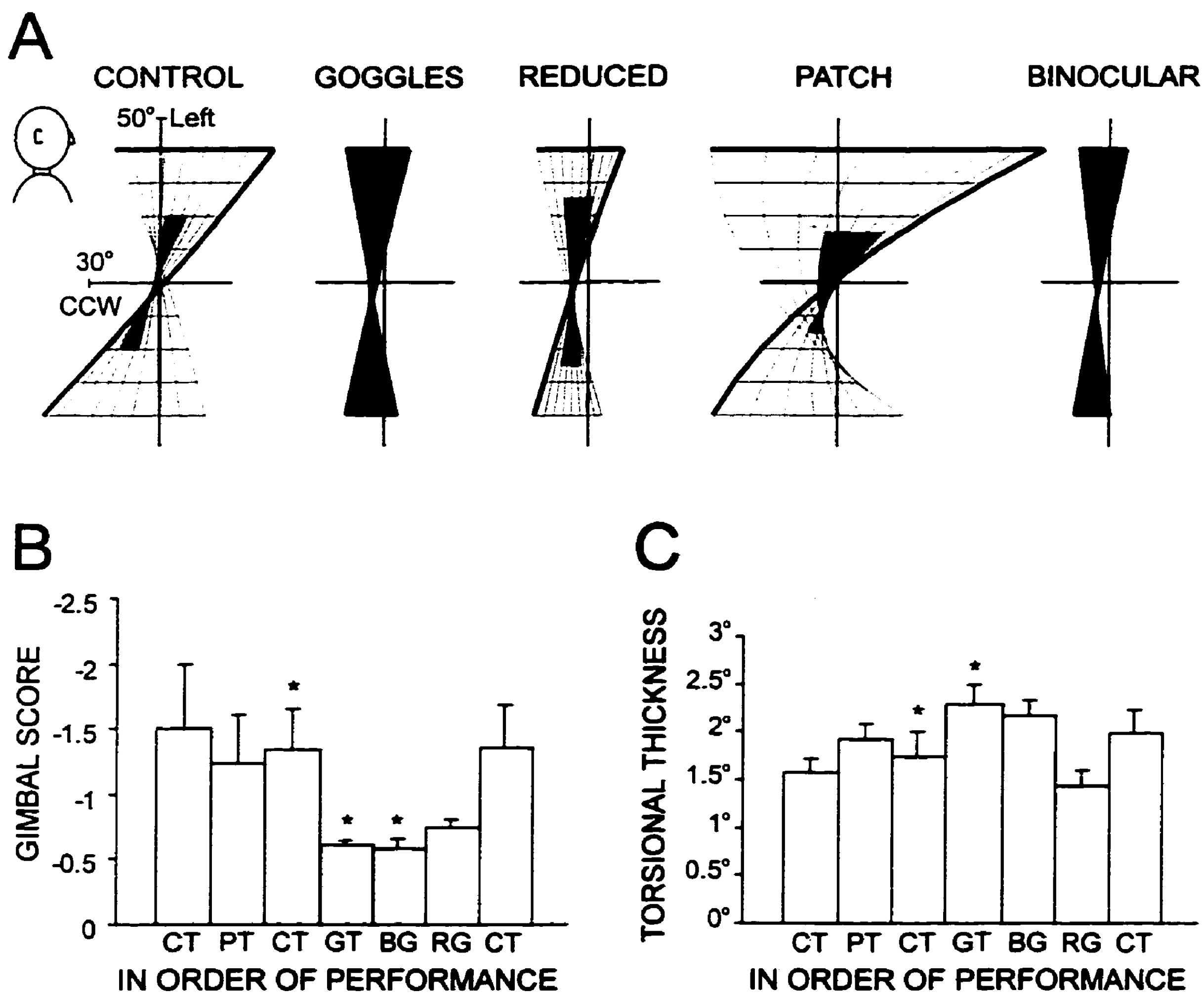

Figure 11. Comparison of 3-D head orientation ranges during fixation of the 9 targets during the various task-constrained paradigms of experiment 2. ***A:*** 2nd-order surface fits to head orientation ranges for each of the 5 tasks, viewed from the side of subject. Shaded regions reflect the actual data range with each surface fitted with a 40° X 40° range for standardization. ***B:*** quantitative comparison of the gimbal score. Each bar represents the average gimbal score across all 7 subjects with standard error, for each paradigm presented in order of performance (100s intervals): CT, control; PT, left-eye patch; GT, goggle; BG, binocular goggle; RG, reduced head range. * indicates significance ($p < .05$, two-tailed) relative to control condition. ***C:*** quantitative comparison of the torsional thickness score of the head orientation range to the fitted surface. Each bar represents the average torsional thickness score, in degrees, across all 7 subjects with standard error, for each paradigm presented in order of performance (100s intervals) with the above designations. * indicates significance ($p < .05$, two-tailed) relative to control condition.

experiment 1, a flattened surface with a slight twist. When the average amount of twist in the goggles condition across all subjects was quantified for this experiment (figure 11B), the resulting gimbal score (-.581) was again significantly lower than that of the control (-1.436; $P < .036$ as denoted by the asterisk).

Therefore, the rest of our analysis was designed to determine which task constraint was altering Donders' law in goggles paradigm. The large head range made with the goggles during the standard goggles condition was controlled for by reducing the range of the targets to a range defined by final head positions in the control condition. Subjects made gaze shifts as instructed before but to 9 targets that were now placed (same pattern as standard range) at retinal distances of 25° horizontal and 20° vertical. This range was utilized to reflect the typical head range used by subjects in the control condition of the first experiment. If the flattening of the surface was a by-product of an increase in head range, then by decreasing this range one should expect a Fick-gimbal like twist of the reduced head range surface. The surface of best fit for the reduced range resembles a Fick-gimbal that is somewhat flattened (fig. 11A, reduced). When the gimbal score for the reduced range (-.611) was compared relative to the control (-1.436), there was a large decrease that approaches significance ($p \geq .089$). Although the gimbal score of the reduced range is not statistically significant compared to the control condition (probably because the reduction in the range yields more variable fits), in comparison to the control condition the calculated amount of twist is less than half and similar to the full range.

If the loss of input from one eye is the cause of the flattening of the surface in the goggles condition, one would expect a similar flattening of the surface in the monocular task. However, the shape of the surface in the left-eye patch condition (fig. 11A, patch) was generally similar to the control task in that the surface was twisted in the direction indicative of a Fick-gimbal (although, in this example the twist was increased and the vertex of the twist was shifted slightly in the CCW direction). The corresponding average gimbal score, -1.229, for the patch ("PT") in (B) suggests that the head was adhering to the Fick-gimbal constraint almost as much as the control. The average score did decrease slightly, compared to the control, but this decrease was not significant ($p \geq .415$).

To further investigate the possible role of binocular cues without peripheral vision, subjects were asked to wear goggles with apertures in both visual hemifields (binocular condition, "BG"). If one assumes that the loss of binocular visual input is the cause of the flattening of the surface observed in the goggles condition, then one should expect a surface with a Fick twist in this condition. In figure 11A (binocular fit), there was a flattening of the surface in the binocular goggles task similar to the standard goggles condition. When the amount of twist in this surface was quantified (fig. 11B, "BG"), the gimbal score (-.581) was significantly lower compared to the control (-1.436; asterisk denotes significance, $p < .031$), suggesting that the surface was flatter than a surface generated by a Fick-gimbal system. In addition, the gimbal score for the binocular goggles was almost identical to the monocular goggles condition (by only

.0003 difference). The results from this paradigm and the left-eye patch paradigm suggest that the loss of input from one eye, resulting from the standard goggles, does not explain the flattening of the surface in the goggles condition in experiment 1 and experiment 2.

Thus far only the form of Donders' law in experiment 2 has been discussed without addressing the more fundamental question of whether it was obeyed. Recall that from experiment 1 the measure of torsional thickness or variance of a surface was a good measure of whether final *Hs* positions systematically adhered to the surface of best fit, or in other words, how well Donders' law was obeyed. Figure 11C is the graphical representation (across subjects) of task constraints (x axis) and their corresponding average torsional thickness in degrees (y axis). The only significant difference in the torsional thickness as compared to the control was found for the goggles condition ($p < .005$). The reduced range condition and binocular goggles condition approached significance ($p \leq .066$ and $p \leq .051$ respectively). In the standard range goggle condition, the average torsional thickness increased slightly to 2.23°, similar to the average torsional thickness score of the goggle task in experiment 1. However, in the reduced range condition the average torsional thickness score significantly decreased (1.45°). Thus for a given range of head positions, Donders' law was adhered to at least as well if not better in the goggle conditions then in normal controls.

In summary, the findings argue against the hypotheses that the flattening was due to a general degradation effect, a trivial range effect, or the loss of binocular vision.

However, two reasonable hypotheses remained: (1) that the effect was due to a loss of peripheral vision (i.e. a loss of visually orienting information in the environment); or (2) a neuro-motor effect involving the change in the role of the head during gaze shifts (figures 6 and 7). Testing between these hypotheses was the subject of the next experiment.

Peripheral Vision vs. Motor coordination. To determine if Donders' law has something to do with orienting the peripheral visual field to features of the environment, and that the pinhole goggles flattened the H_s surface by blocking out the periphery, a task was devised that had the same motor requirements as the goggles task, but allowed for full peripheral vision. This was done by having subjects point a laser mounted on a helmet to targets of the standard range (i.e. 40° horizontal/vertical). If peripheral vision played a role in the flattening of the head range surface, the flattening observed during the goggles paradigm should disappear during the laser paradigm (which permits visual input from the periphery) in favor of a Fick-gimbal like surface. Figure 12A ("control-helmet") is the 2-D surface fit for the control condition in which subjects made normal eye-head gaze shifts to the targets of the standard range with the helmet on, laser turned off. The resulting surface is twisted in the normal Fick-gimbal like manner with a gimbal score of -0.890, with the range of final head positions (darkened portion) similar to the control conditions of the previous two experiments (figures 9C and 11A).

During the laser paradigm, subjects were required to point the laser at targets of the standard range. Figure 12A ("laser") is the 2-D surface of best fit for the laser

Figure 12

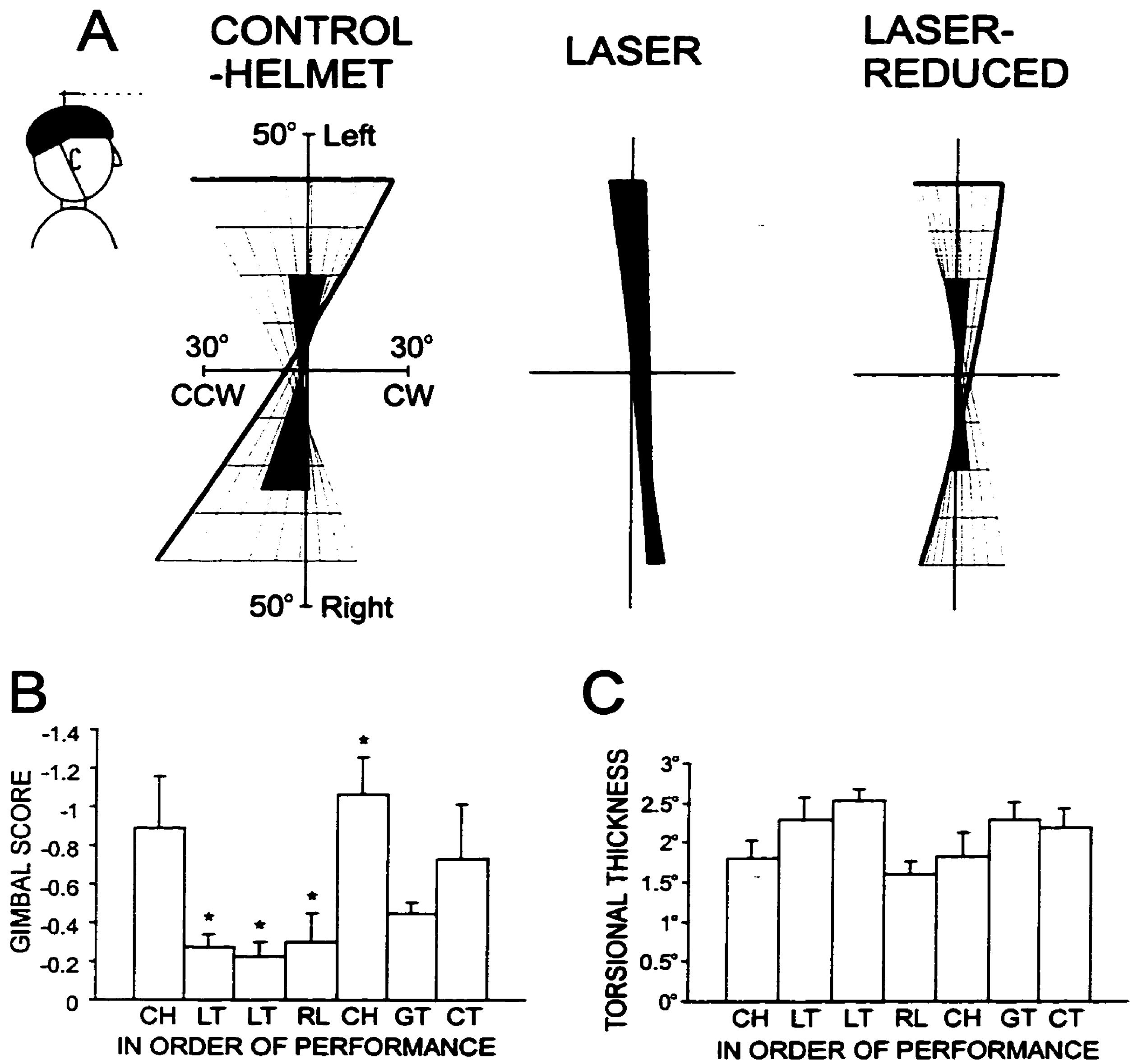

Figure 12. 3-D head orientation ranges during fixation of the 9 targets during the various task-constrained paradigms of experiment 3. ***A:*** 2nd-order surface fits to head orientation ranges viewed from the side of subject M.S. for control-helmet condition; laser condition; and laser-reduced condition. Shaded regions reflect the actual data range with each surface fitted with a 40°X 40° range for standardization. ***B:*** quantitative comparison of the average gimbal score. Same convention as figure 9 with the following designations: CH, control helmet; LT, laser; RL, laser-reduced; GT, goggle; CT, control. ***C:*** quantitative comparison of the average torsional thickness score of the head orientation range to a 2nd-order surface. Same convention as figure 11 with the above designations.

condition as viewed from the side. Note that in the figure the surface is markedly flat and extends the full ● 40°. The corresponding average gimbal score, figure 12 ("LT"), showed a noticeable drop down to -0.248 (averaged across both trials). The laser paradigm gimbal scores were highly significant when compared to the control condition ($p \leq .007$ for the first laser, $p \leq .010$ for the second laser). Thus it appeared that the loss of peripheral vision during the goggles conditions was not the causing factor of the flattening effect.

To check for range effects, subjects were instructed to land the laser on targets of the reduced range. Figure 12A ("laser-reduced") is the second order surface fit to final head positions for the laser reduced range condition. The surface, similar to that for the goggles reduced condition in figure 11A, was flattened with a slight twist. When the twist was quantified, as shown in figure 12B ("RL"), the resulting average gimbal score of -.303 for this condition was only slightly larger than the standard laser scores ("LT"), but highly significant ($p \leq .021$) when compared to the control condition ("CH"). In addition, this score was slightly lower than the goggle scores ("GT"), done as a further control.

Figure 12C illustrates graphically the individual torsional thickness scores of the various conditions (i.e. control-helmet, laser, laser-reduced, goggles and control). When the various tasks (i.e. laser, laser-reduced, and goggles) were compared relative to the control helmet and control conditions, there were no significant changes in the amount of torsional thickness (across subjects). However, a trend similar to that observed in experiment 2 was noticed. Relative to the control-helmet condition, the torsional thickness scores for the 2 laser paradigms increased, and the score decreased for the reduced laser paradigm. The increase observed in the laser conditions (fig. 12C "LT"), relative to control helmet, and goggles condition (fig. 12C "GT"), relative to control, were found to be non significant and as such lend credence to the notion that Donders' law is obeyed under all gaze directing task conditions. In other words, it appears that Donders' law of the head subserves the gaze motor control system. If this were true, then one would hypothesize that when the head is required to perform a task other than moving the line of sight, Donders' law should break down. This was the aim of our next experiment.

Adherence to Donders' law during head-gaze dissociation. In the first three experiments, gaze was consistently driven to the target, whether through normal eye-head coordination (control, patch, dark, control-helmet) or mostly through head movement (goggles and laser paradigms). To determine whether the head motor control system specifically optimizes for Donders' law for the purpose of shifting gaze, a fourth experiment was designed during which subjects fixated their gaze on a center target and moved the laser to illuminate the targets of the reduced range. This gaze fixation task provided a means of dissociating the head from gaze such that the head moved but not to redirect gaze. In this case it is hypothesized that Donders' law should break down.

Figure 13

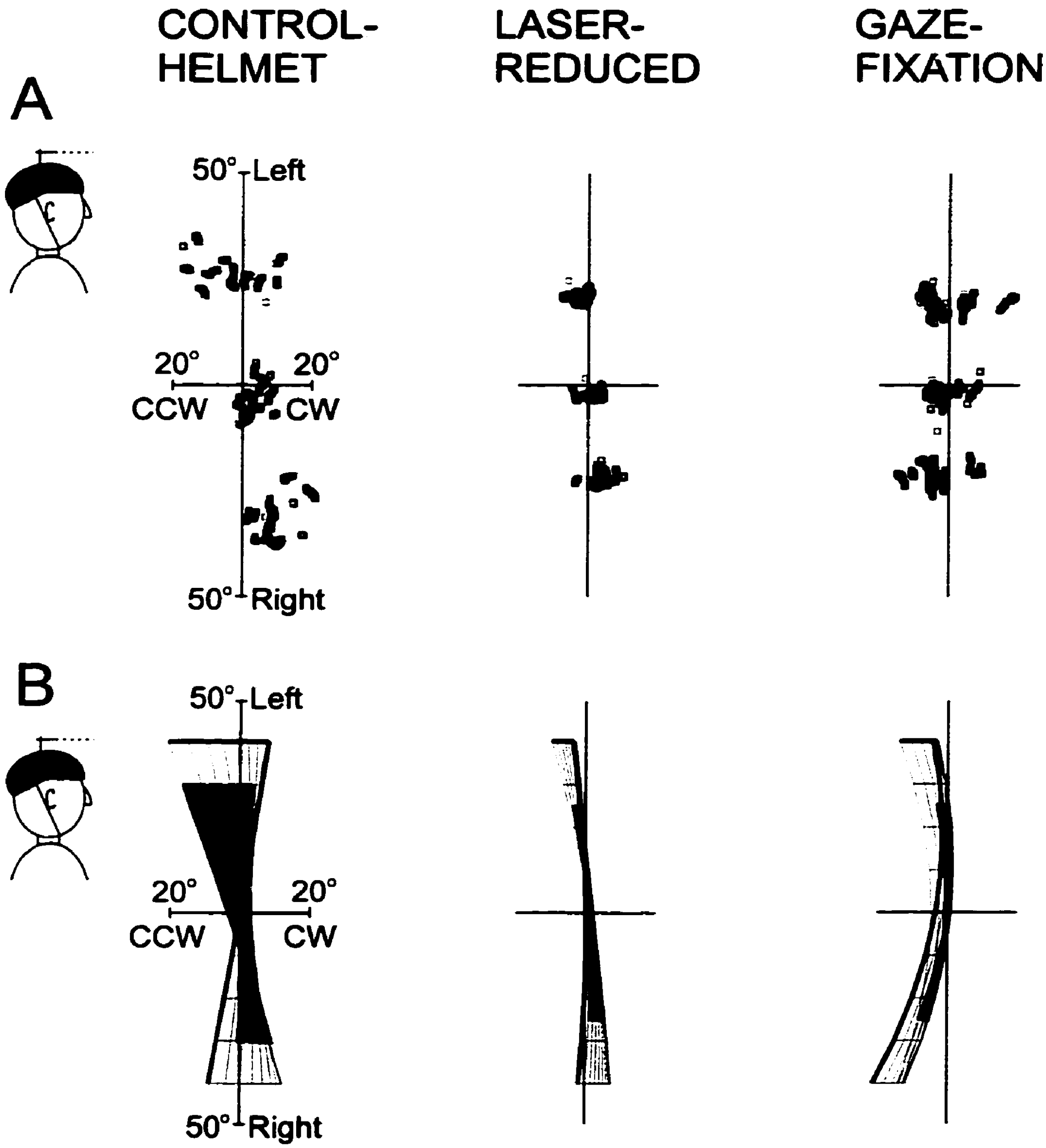

Figure 13. 3-D head orientation ranges during fixation of the 9 targets during the various task-constrained paradigms of experiment 4. ***A:*** quaternion vectors plotted according to the right-handed rule from the side perspective for subject S.P. for control-helmet; laser-reduced; and gaze-fixation conditions. ***B:*** 2nd-order surface fits to the same head orientation ranges in ***A***. Shaded regions reflect the actual data range with each surface fitted with a 40° X 40° range for standardization.

Figure 13 plots the control-helmet, laser-reduced, and gaze-fixation conditions as data plots (A) and second order surfaces of best fit (B) from the side perspective for one subject during unrestricted gaze shifts. The control-helmet and laser-reduced conditions were performed in the same manner as in the previous experiment. In the control condition (fig.13B, "control-helmet"), the resulting 3-D surface was twisted in the Fick-gimbal direction with an average gimbal score (across subjects) of -.964 ("CH" in fig. 14A). Figure 13A ("laser-reduced") is the plot of final head positions for the laser-reduced range condition. The range is defined by the 25°/20°/28° (horizontal/vertical/oblique respectively) target range and is denoted by the shaded portion of figure 13B ("laser-reduced"). The corresponding average gimbal score for the laser-reduced condition ("LR" in fig. 14A), -.457 ($p < .029$, one-tailed), was significant relative to the control (similar to that quantified in the laser-reduced condition of the previous experiment). The gimbal score for the gaze-fixation condition ("GF" in fig. 14A) was -.290. This score was significantly lower relative to the control condition ($p \leq .005$) and markedly flat in comparison (fig. 13B, "gaze-fixation"). Again, this could be due to a change in Donders' law, a degradation of Donders' law, as hypothesized, or both.

To test between these possibilities, torsional thickness scores of the fitted surfaces for all three conditions were calculated and are illustrated in figure 14B. For the control-helmet condition, an average score of 1.863° was obtained which was relatively similar to that of the previous experiment. As expected, the average torsional thickness score of the laser-reduced condition, 1.585°, was lower than that of the control-helmet condition. This

Figure 14

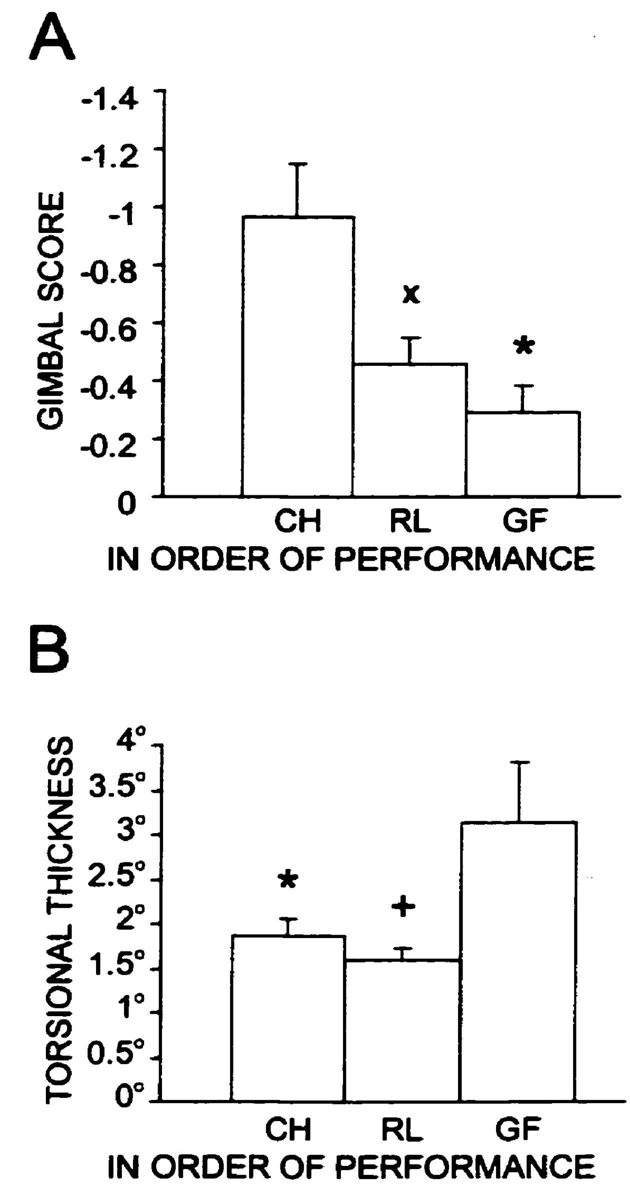

Figure 14. Quantitative comparison of the gimbal and variance scores for head orientation ranges of experiment 4. ***A:*** quantitative comparison of the average gimbal score. Same convention as figure 11 with the following designations: CH, control-helmet; RL, laser-reduced; GF, gaze-fixation. * indicates significance ($p < .05$, two-tailed) relative to the control helmet; x indicates significance ($p < .05$, one-tailed) relative to control helmet. ***B:*** quantitative comparison of the average torsional thickness score of the head orientation range to a 2nd-order surface. Same conventions as figure 11 with the above designations. * indicates significance ($p < .05$, one-tailed) relative to the control helmet; + indicates significance ($p < .05$, one-tailed) relative to laser-reduced condition.

can be seen in figure 13B, where final head positions are tightly grouped about the torsional axis. If Donders' law is degraded as a consequence of moving the head without redirecting gaze, as hypothesized, then the torsional thickness score should be higher in the gaze-fixation condition than in the laser-reduced and control-helmet conditions. Visually, in figure 13A ("gaze-fixation"), final head positions are much more scattered along the torsional axis suggesting a weak adherence to the fitted surface (fig. 13B, "gaze-fixation"). When this scatter was quantified, an average torsional thickness score of 3.135° was calculated, which was significant ($p = .029$, one-tailed, relative to the laser reduced condition; $p = .031$, one-tailed, relative to the control helmet condition). This suggests that when the head is not used to redirect gaze, the Donders' law constraint is relaxed.

To understand this relaxation of Donders' law, the axes of head rotation were examined. If in the gaze-fixation paradigm the head motor system was using Listing's law, as the gimbal score suggests, the axes of rotation should tilt out of Listing's plane (which would be aligned with the vertical axis of the coils) by half the angle of rotation. Figure 15 shows the facing directions of the head, and the corresponding axes of rotation shown as velocity loops for leftward and rightward movements to the left and right targets of the reduced range at each of the three vertical levels (up, middle, and down targets; see figure 5 for target locations). As Fig. 15A–C shows, these axes lay roughly orthogonal to the facing direction, a pattern which is inconsistent with Fick (where they would line up with the fixed vertical axis in all three cases) or Listing (where they would

Figure 15

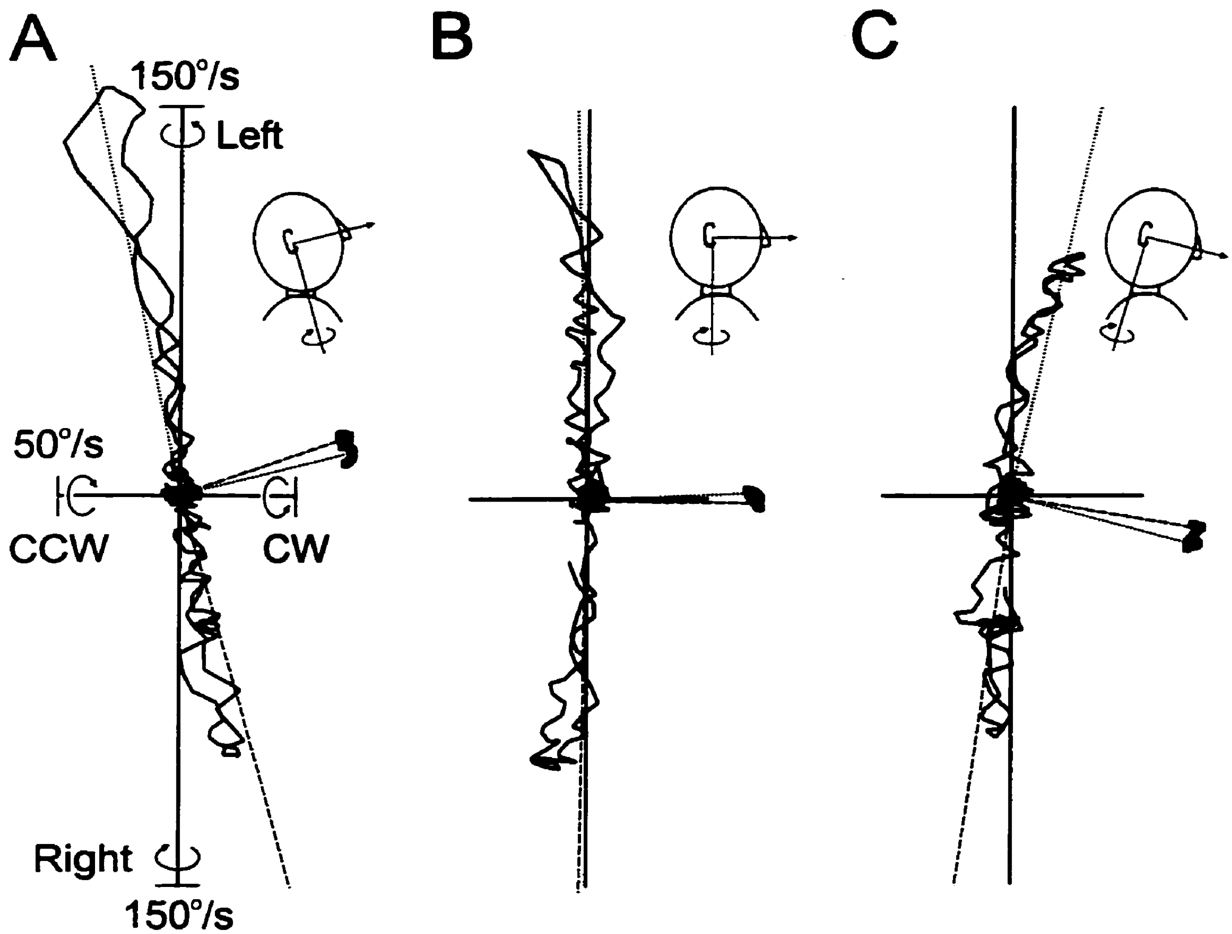

Figure 15. Minimum rotation strategy observed during the head-gaze dissociation task. ***A***: Head facing upward targets. ***B***: Head facing forward targets. ***C***: Head facing downward targets. Each panel shows two oppositely elongated (one upward and one downward) angular velocity loops - for one leftward and one rightward head movement respectively. Each point along these loops defines the instantaneous axis and speed of head rotation, as a vector emanating from the origin. Vectors pointing rightward (i.e., forward for the subject) show the facing direction of the head during the rightward (----) and leftward (.....) movements. Corresponding vertical lines show the perpendiculars to these facing vectors, which aligned closely with the angular velocity loops. Thus, as indicated by the caricatures, the vertical axis of head rotation remained orthogonal to head facing direction, in contrast to the space-fixed vertical axes observed during normal random gaze shifts.

tilt by half the amount), and indeed with any form of Donders' law, but which transports the facing direction using the smallest possible head rotation (see Tweed and Vilis 1990). This strategy is similar to the minimum-rotation strategy observed by Tweed and Vilis (1992) where subjects abandoned Donders' law for a quicker strategy during repetitive horizontal movements. By using the miminum-rotation strategy, the deviations from Donders' law cancel out across randomly directed movements, producing the thick, flat distribution shown in Fig. 13B ("gaze-fixation").

H_s torsional position as a function of horizontal and vertical position. Up until this point, only the fits of the head range along a continuum of ideal gimbal scores have been quantified. However, the more general shifts, tilts, or curves in these ranges have yet to be examined. To determine if such additional parameters were necessary to describe the effects of our various tasks, the six coefficients of a 2[nd] order surface fit were quantified (equation 2). These six parameters measure the dependency of torsion on horizontal and vertical position (Glenn and Vilis, 1992; Medendorp et al, 1998; Crawford et al, 1999). Figure 16 illustrates the six a values for each of the task constraints (A - I) for 7 subjects sampled from the 4 experiments. Each bar represents the average score for each a value and standard error. The first a value, a_1, describes the amount of torsional shift of the range from a reference position. The average a_1 scores were consistently small (ranging from -.009 to .0042) and never significantly different from 0. The second parameter, a_2, describes the dependence of torsion on vertical Hs positions (horizontal rotational axis).

Figure 16

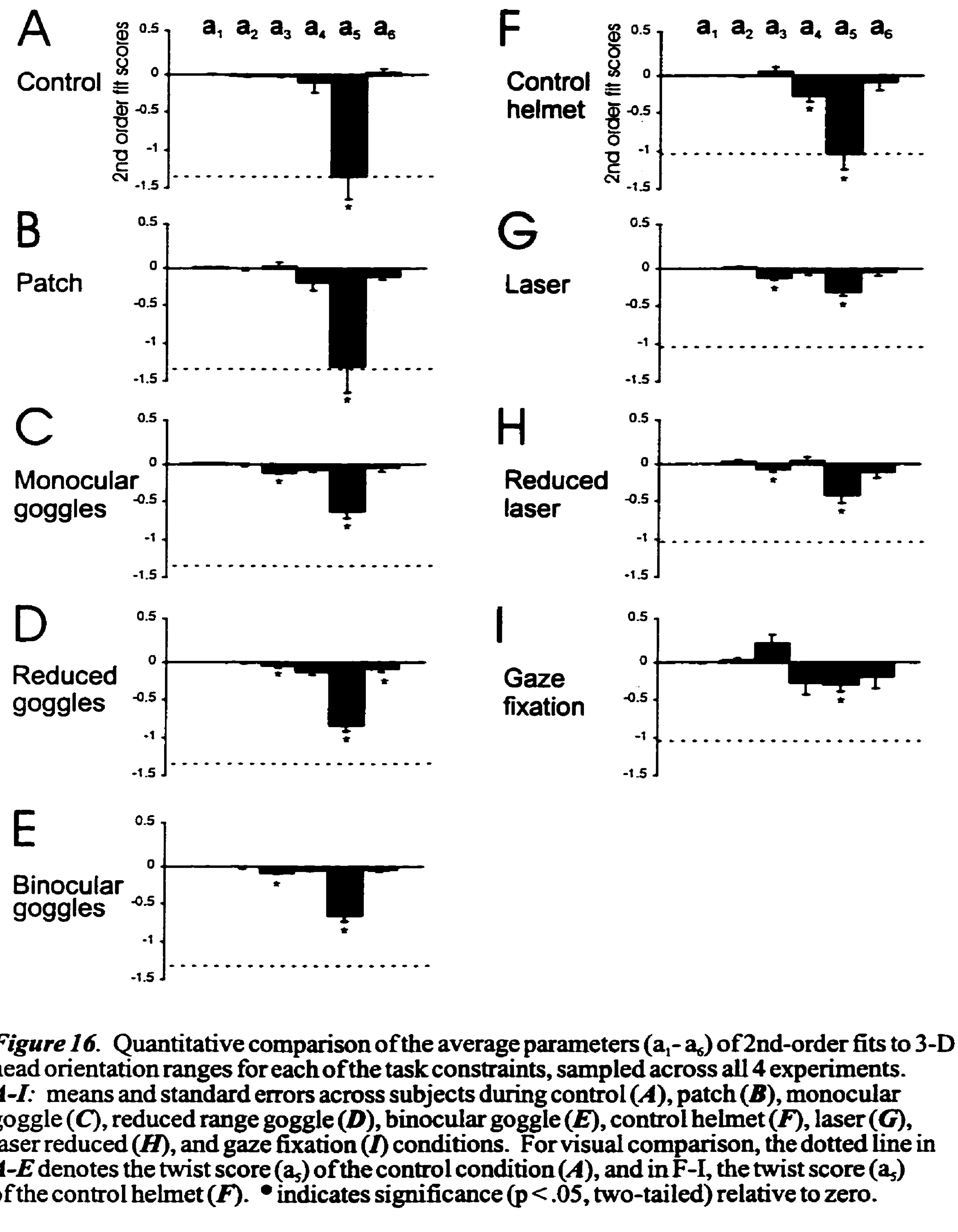

Figure 16. Quantitative comparison of the average parameters (a_1 - a_6) of 2nd-order fits to 3-D head orientation ranges for each of the task constraints, sampled across all 4 experiments. *A-I:* means and standard errors across subjects during control (*A*), patch (*B*), monocular goggle (*C*), reduced range goggle (*D*), binocular goggle (*E*), control helmet (*F*), laser (*G*), laser reduced (*H*), and gaze fixation (*I*) conditions. For visual comparison, the dotted line in *A-E* denotes the twist score (a_5) of the control condition (*A*), and in F-I, the twist score (a_5) of the control helmet (*F*). • indicates significance ($p < .05$, two-tailed) relative to zero.

These average a_2 scores were also consistently small across tasks (range of -.013 to .025) and never significant. The a_3 scores, dependence of torsion on horizontal Hs position, had a slightly larger range across tasks (-.118 to .239) and was significantly different from zero in: goggles paradigms, figures 16C (-.107; $p < .0015$), 16D (-.050; $p < .034$), and 16E (-.079; $p < .0073$); and laser paradigms, figures 16G (-.118; $p < .0054$) and 16H (-.078; $p < .043$). The negative scores describe the backward tilt observable in figures 12A ("laser") and 13B ("laser-reduced"), reflecting that rightward positions tended to be more clockwise.

The fourth parameter, a_4, describes the curvature along the torsional axis with vertical eye position. The range of a_4 scores (-.269 to .03) was still relatively small across paradigms and non-significant, with the exception of the control helmet paradigm (fig. 16F), where the score was significantly different from zero (-.269; $p < .0092$). This negative score reflects the tendency of the head to tilt in the counterclockwise direction when assuming upward and downward positions. The sixth parameter, a_6 scores, describes the curvature along the torsional axis with horizontal eye position. As with the fourth a parameter, the range of a_6 scores (-.192 to .022) was small across tasks with significance from zero for only one paradigm, reduced goggles, 16D, (-.09; $p \leq .046$). This negative value describes the tendency of the head to tilt counterclockwise when looking left and right, as can be seen in figure 13B ("gaze-fixation" paradigm).

Finally, the fifth term, a_5, describes the twist of the surface of Hs position vectors. This score is highly related to the gimbal score used across all our subjects and tasks.

This "twist score" was clearly the dominant *a* term (in terms of being largest) and was consistently negative, signifying a Fick-gimbal like twist. This score was the only score that was consistently significant (from zero) for all paradigms and showed the greatest variation between paradigms (range). This suggests that the gimbal score used in figures 10 through 14, captured the vast majority of the effect induced by our various paradigms.

DISCUSSION

The eye and the head are both capable of rotating in any of the three dimensions, i.e. horizontal, vertical, and torsional. This poses a kinematic redundancy problem which must be resolved in order for the gaze motor control system to convert a 2-D retinal input into a 3-D motor output command for the eye and head. Originally, Donders' law stated that for any given gaze direction the eye assumed a unique 3-D orientation (Donders, 1847) thereby minimizing rotation around the torsional dimension (as dictated by Listing's law) and maintaining final eye position within a plane, i.e. Listing's plane (Helmholtz, 1877; Ferman et al, 1987; Tweed and Vilis, 1990). The head motor system appears to abide by the same law but is implemented not by Listing's law by rather a Fick-gimbal strategy during normal eye-head gaze shifts (Glenn and Vilis, 1992; Radau et al, 1994; Misslisch et al, 1998). However, prior to this study there was no direct evidence to indicate why one of these choices was made over the other.

Purpose of Donders' Law. Does the gaze motor control system always optimize for Donders' law? It has been suggested that the head motor system specifically optimizes for Donders' law for the purpose of gaze control (Tweed, 1997; Crawford et al, 1999). The torsional thickness scores in the first three experiments of this study suggested that when the primary purpose of the gaze system was to redirect gaze, regardless of the relative contributions of the head and eye, Donders' law is consistently obeyed. For instance, when subjects donned the pin-hole goggles, the head became the prime mover of the gaze line. Similarly, when the helmet-mounted laser was used to redirect gaze, the head was solely responsible for pointing the beam at the targets. The head motor system abandons the Fick strategy when it becomes the prime mover of gaze for a strategy that takes the fastest route, Listing's strategy, but still ensures that torsion does not accumulate (by obeying Donders' law). Thus it appears that the motor system specifically optimizes Donders' law of the head by using it as a platform for the purpose of shifting the line of sight.

Although it appears that Donders' law is consistently obeyed by the head, the head motor system itself can repeal the law when the task requirements change. For example, humans can voluntarily move their heads to any position they choose (within skeletomuscular constraints, of course; Tweed, 1997), e.g. nodding their heads or shaking them without having to necessarily redirect gaze. In this study, this was induced in our subjects by having them move their heads while their gaze remained fixed on a central target. In this instance, Donders' law broke down in favor of a minimum-rotation strategy that allowed for faster movement of the head by rotating the head about an axis that is orthogonal to the facing direction (figure 15), and hence which allowed for torsion to accumulate (as evidenced by the large torsional thickness score, "GF", in figure 14B).

Purpose of Fick-gimbal vs. Listing's law. This study and previous studies (Tweed and Vilis, 1992; Radau et al, 1994; Crawford and Guitton, 1997; Crawford et al, 1999) have determined that Donders' law of the head is controlled neurally and is most likely to be task constrained since the strategy used to implement it can be switched according to the task. For instance, when subjects wore the helmet-mounted laser, Listing's law became the more efficient strategy because it was able to redirect the facing direction using the smallest possible rotations (about a fixed-axis in Listing's plane) toward and away from some central, primary position (see figure 3). This allows for the quicker aiming action of the laser. In contrast, when the head is used as a platform, as in "normal" gaze shifts, its role is smaller in comparison and thus is able to optimize other variables (such as work done against gravity).

Consider a Donders' law continuum, which is bounded on one end by the Fick strategy (gimbal score of −1) and on the other end, a Helmholtz strategy (gimbal score of +1), with Listing's law in the middle (Crawford and Vilis, 1995; Glenn and Vilis, 1992). To accommodate task requirements (and skeletomuscular constraints), the gaze system would select a point/rule along this continuum to best uphold Donders' law during gaze directing movements. An example of this is the goggle paradigm of the present study, where the gaze motor control system may have selected to implement Donders' law through a strategy intermediate between a Fick and a Listing's, as evidenced by the gimbal score. The question then is what leads to the choice of which point on the continuum is chosen?

Several possible explanations have been proposed as to what constraints are being optimized by the gaze motor control system. This was done by differentiating peripheral vision effects (goggles paradigms), binocular vision effects (left eye patch and binocular goggle paradigms), mechanical effects (reduced head range), and motor role of the head (laser paradigms). Figures 11A and 12A illustrate the surfaces of best fit for final *Hs* positions under each of the above bracketed task constraints. The gimbal scores (figures 11B and 12B) for the goggle paradigms significantly decreased relative to the control condition (i.e. flattening of the normally twisted Fick-like surface), and as such it was initially hypothesized that either peripheral vision or the change in the motor role of the head (from platform to pointer) determined the strategy used by the gaze motor system in order to adhere to Donders' law. To reconcile which of the two hypotheses (i.e. peripheral vision or motor role of the head) was valid, the two effects were dissociated and tested separately. The laser paradigms duplicated the head movement observed in the goggle condition but allowed for peripheral vision. The gimbal score remained low relative to the control suggesting that the flattening of the Fick-gimbal surface observed during the goggles condition (figure 9D) was not due to the loss of peripheral vision, rather it was likely due to the change in the head's motor role. That is when the line of sight is to be shifted and the range of eye movement is limited (as is the case with goggles), the gaze control system abandons the "normal" role of using the head as a platform for eye movement (which is now restricted) for one that makes the head the pointer, the main mover of gaze, while still upholding Donders' law. In the case of the goggles task, it appears to be an intermediate point along the continuum between Listing's and Fick.

Role and neural mechanism of Donders' law operator in gaze shifts. Recently it has been suggested that within the superior colliculus there is a map that specifies desired gaze movement, i.e. dynamic 2-D gaze error (Tomlinson and Bahra, 1986; Galiana and Guitton, 1992; Freedman and Sparks, 1997; Goosens and Van Opstal, 1997). It has been suggested that this gaze signal is sent from the superior colliculus down the brainstem circuit where it decussates into separate eye and head commands (Freedman and Sparks, 1996). The 2-D gaze error signal for the head would then be converted by a Gimbal operator (constrained by Donders' law) into a 3-D motor output command which would then be sent to the head motor plant (Tweed et al, 1997). The role of the gimbal operator is essential in determining final head position for, as discussed, there are an infinite number of orientations the head can assume about the torsional axis for every single gaze direction.

If one considers the results of the fourth experiment, the 2-D gaze command that would have to arise in the superior colliculus would be zero since, in the gaze fixation paradigm, gaze is fixed. Therefore the command for the head movement observed can not come from the superior colliculus but rather from an alternative source along an alternate parallel pathway(s) that likely involves other structures, such as the motor cortex or the basal ganglia, which apparently bypasses the Donders' Law operator (Medendorp, 1999) providing another, separate 3-D head position signal.

General implications and conclusions. Understanding the kinematics underlying gaze movements has been an important step in unraveling the mysteries of general motor control. Principles that guide the gaze system are similar to those found to in other components of the motor system such as reaching. Donders' law is one example. This study focused on Donders' law of the head (in addition to Glenn and Vilis, 1992; Radau et al, 1994; Tweed et al, 1995; Misslisch et al, 1998) and other studies have focused on the eye (Helmholtz, 1867; Ferman et al, 1987; Tweed and Vilis, 1990) and the arm (Straumann et al, 1991; Hore et al, 1992; Theeuwen et al, 1993). The strategies that are implemented in accordance to Donders' law are neural in nature and may be different for each system (i.e. Listing's law for the eye, Fick-gimbal for the head and arm). However, by adhering to Donders' law, the brain may be simplifying a complex system and providing a framework within which each system is able to interact and ultimately execute a coordinated movement. Although the constraints within each of the motor systems are not completely understood, this study has attempted to elucidate those constraints that determine the strategy, i.e. Fick-gimbal vs. Listing's law, used by the head motor system in adherence to Donders' law. Results from this study suggest that the motor role of the head in the redirection of gaze is most likely one of the underlying constraints.

REFERENCES

Bernstein, N. (1967). The coordination and regulation of movements. Oxford: Pergamon Press.

Buttner, U., Buttner-Ennever, J.A., and Henn, V. (1977). Vertical eye unit related activity in the rostral mesencephalic reticular formation of the alert monkey. Brain Research, 130, 239-252.

Cannon, S.C., and Robinson, D.A. (1987). Loss of the neural integrator of the oculomotor system from brainstem lesions in the monkey. Journal of Neurophysiology, 57, 1383-1409.

Crawford, J.D. (1994). The oculomotor neural integrator uses a behavior-related coordinate system. Journal of Neuroscience, 14, 6911-6923.

Crawford, J.D., Cadera, W., and Vilis, T. (1991). Generation of torsional and vertical eye position signals by the interstitial nucleus of Cajal. Science, 252, 1551-1553.

Crawford, J.D., Ceylan, M.Z., Klier, E.M., and Guitton, D. (1999). Three-dimensional eye-head coordination during gaze saccades in the primate. Journal of Neurophysiology, 81, 1760-1782.

Crawford, J.D., and Guitton, D. (1997). Primate head-free saccade generator implements a desired (post-VOR) eye position command by anticipating intended head motion. Journal of Neurophysiology, 78, 2811-2816.

Crawford, J.D., and Vilis, T. (1991). Axes of eye rotation and Listing's law during rotations of the head. Journal of Neurophysiology, 65, 407-423.

Crawford, J.D., and Vilis, T. (1995). How do motor systems deal with the problems of controlling three-dimensional rotations? Journal of Motor Behavior, 27, 89-99.

Donders, F.C. (1847). Beitrag zur Lehre von den Bewegungen des menschlichen Auges. Holland. Beit. Anatom. Physiolog. Wiss., 1, 105-145.

Ferman, L., Collewijn, H., and Van Den Berg, A.V. (1987). A direct test of listing's law. I. Human ocular torsion measured in static tertiary positions. Vision Research, 27, 929-938.

Freedman, E.G., Stanford, T.R., and Sparks, D.L. (1996). Combined eye-head gaze shifts produced by electrical stimulation of the superior colliculus in rhesus monkeys. Journal of Neurophysiology, 76, 927-952.

Freedman, E.G., and Sparks, D.L. (1997a). Eye-head coordination during head unrestrained gaze shifts in rhesus monkeys. Journal of Neurophysiology, 77, 2328-2348.

Freedman, E.G., and Sparks, D.L. (1997b). Activity of cells in the deeper layers of the superior colliculus of the rhesus monkey: Evidence for a gaze displacement command. Journal of Neurophysiology, 77, 1669-1690.

Fukushima, K., Harada, C., Fukushima, J., and Suzuki, Y. (1990). Spatial properties of vertical eye movement-related neurons in the region of the interstitial nucleus of Cajal. Experimental Brain Research, 79, 25-42.

Galiana, H.L. (1990). Oculomotor Control. In D.N. Osherson, S.M. Kosslyn, and J.M. Hollerbach (Eds), Visual Cognition and Action (pp. 243-283). Cambridge, USA: MIT Press.

Galiana, H.L., and Guitton, D. (1992). Central organization and modeling of eye-head coordination during orienting gaze shifts. Ann. NY Acad. Sci., 565, 452-471.

Galiana, H.L., Guitton, D., and Munoz, D.P. (1992). Modeling head-free gaze control in the cat. In A Berthoz, W Graf, and PP Vidal (Eds.), The Head-Neck Sensory-Motor System (pp. 520-525). New York: Oxford UP.

Glenn, B., and Vilis, T. (1992). Violations of listing's law after large eye and head gaze shifts. Journal of Neurophysiology, 68, 309-318.

Goffart, L., and Pelisson, D. (1998). Orienting gaze shifts during muscimol inactivation of caudal fastigial nucleus in the cat. I. Gaze dysmetria. Journal of Neurophysiology, 79, 1942-1958.

Goffart, L., Pelisson, D., and Guillaume, A. (1998). Orienting gaze shifts during muscimol inactivation of caudal fastigial nucleus in the cat. II. Dynamics and Eye-head coupling. Journal of Neurophysiology, 79, 1959-1976.

Goldberg, M.E., Eggers, H.M., and Gouras, P. (1991). The ocular motor system. In E.R. Kandel, J.H. Schwartz, and T.M. Jessell (Eds), Principles of Neuroscience (pp. 661-678). Norwalk, CT: Appleton and Lange.

Goldberg, M.E., and Wurtz, R.H. (1972). Activity of the superior colliculus in behaving monkeys. II. Effect of attention on neuronal colliculus responses. Journal of Neurophysiology, 35, 560-574.

Goosens, H.H.L.M., and Van Opstal, A.J. (1997). Human eye-head coordination in two dimensions under different sensorimotor conditions. Experimental Brain Research, 114, 542-560.

Harris, L.R. (1980). The superior colliculus and movements of the head and eyes in cats. Journal of Physiology (London), 300, 367-391.

Hering, E. (1868). Die Lehre vom Binocularen Sehen. Leipzig: Engelmann.

Hollerbach, J.M. (1990). Fundamentals of Motor Behavior. In: D.N. Osherson, S.M. Kosslyn, and J.M. Hollerbach (Eds.), Visual Cognition and Action (vol 2 pp.153-182). Cambridge, Massachusetts: MIT Press.

Hore, J., Watts, S., and Vilis, T. (1992). Constraints on arm position when pointing in three dimensions: Donders' law and the Fick Gimbal strategy. Journal of Neurophysiology, 68, 374-383.

Keller, E.L. (1974). Participation of the medial pontine reticular formation in eye movement generation in the monkey. Journal of Neurophysiology, 37, 316-332.

King, W.M., and Fuchs, A.F. (1979). Reticular control of vertical saccadic eye movements by mesencephalic burst neurons. Journal of Neurophysiology, 42, 861-876.

King, W.M., Fuchs, A.F., and Magnin, M. (1981). Vertical eye movement-related responses of neurons in midbrain near interstitial nucleus of Cajal. Journal of Neurophysiology, 46, 549-562.

Klier, E.M., Wang, H., and Crawford, J.D. (1999). Stimulation of the interstitial nucleus of Cajal (INC) produces torsional and vertical head rotations in fick coordinates. Soc. Neurosci. Abstr., Vol. 25, Part 2, p. 1650.

Lushei, E.S., and Fuchs, A.F. (1972). Activity of brainstem neurons during eye movements in alert monkeys. Journal of Neurophysiology, 35, 445-461.

Misslisch, H., Tweed, D., and Vilis, T. (1998). Neural constraints on eye motion in human eye-head saccades. Journal of Neurophysiology, 79, 859-869.

Medendorp, W.P., Melis, B.J.M., Gielen, C.C.A.M., and Van Gisbergen, J.A.M. (1998). Off-centric rotation axes in natural head movements: implications for vestibular reafference and kinematic redundancy. Journal of Neurophysiology, 79, 2025-2039.

Medendorp, W.P., Van Gisbergen, J.A.M., Horstink, M.W.I.M., and Gielen, C.C.A.M. (1999). Donders' law in torticollis. Journal of Neurophysiology (in press).

Moschovakis, A.K., Scudder, C.A., Highstein, S.M., and Warren, J.D. (1991). Structure of the primate oculomotor burst generator II. Medium lead burst neurons with downward on-directions. Journal of Neurophysiology, 65, 218-229.

Nakayama, K. (1975). Coordination of extraocular muscles. In P. Bachy-Rita and G. Lennerstrand (Eds.), Basic Mechanisms of Ocular Motility and Their Clinical Implications (pp. 193-207). Oxford, UK: Pergamon Press.

Nakayama, K. (1983). Kinematics of normal and strabismic eyes. In C.M. Schor and K.J. Ciuffreda (Eds.), Vergence Eye Movements: Basic and Clinical Aspects (pp. 543-564). Boston, MA: Butterworths.

Radau, P., Tweed, D., and Vilis, T. (1994). Three-dimensional eye, head, and chest orientations after large gaze shifts and the underlying neural strategies. Journal of Neurophysiology, 72, 2840-2852.

Richmond, F.J., and Vidal, P.P. (1988). The motor system: joints and muscles of the neck. In B.W. Peterson and F.J. Richmond (Eds.), Control of Head Movement (pp.1-21). N.Y.C., N.Y.: Oxford University Press.

Robinson, D.A. (1972). Eye movements evoked by collicular stimulation in the alert monkey. Vision Research, 12, 1795-1808.

Robinson, D.L., and Jarvis, C.D. (1974). Superior colliculus neurons studied during head and eye movements of the behaving monkey. Journal of Neurophysiology, 3, 533-540.

Rock, I., DiVita, J., and Barbeito, R. (1981). The effect on form perception of change of orientation in the third dimension. Journal of Experimental Psychology: Human Perception and Performance, 7, 719-732.

Straumann, D., Haslwanter, T., Hepp-Reymond, M.C., and Hepp, K. (1991). Listing's law for the eye, head, and arm movements and their synergistic control. Experimental Brain Research, 86, 209-215.

Theeuwen, M., Miller, L.E., and Gielen, C.C.A.M. (1993). Are the orientations of the head and arm related during pointing movements? Journal of Motor Behavior, 25, 242-250.

Tomlinson, R.D., and Bahra, P.S. (1986). Combined eye-head gaze shifts in the primate. II. Interaction between saccades and the vestibuloocular reflex. Journal of Neurophysiology, 56, 1558-1570.

Tweed, D. (1997). Three-dimensional model of the human eye-head saccadic system. Journal of Neurophysiology, 77, 654-666.

Tweed, D., Cadera, W., and Vilis, T. (1990). Computing three-dimensional eye position quaternions and eye velocity from search coil signals. Vision Research, 32, 97-110.

Tweed, D., Glenn, B., and Vilis, T. (1995). Eye-head coordination during large gaze shifts. Journal of Neurophysiology, 73, 766-779.

Tweed, D., and Vilis, T. (1990). Geometric relations of eye position and velocity vectors during saccades. Vision Research, 30, 111-127.

Tweed, D., and Vilis, T. (1992). Listing's law for gaze-directing head movements. In A. Berthoz, W. Graf, and P.P. Vidal (Eds.), The Head-Neck Sensory-Motor System (pp. 387-391). New York: Oxford UP.

von Helmholtz, H. (1867). Torsional translations. In: Treatise on Physiological Optics translated by J.P.C. Southall. Rochester, New York: Opt. Soc. Am., 1925, vol. 3: 44-51.

Westheimer, G. (1957). Kinematics of the eye. Journal of the Optical Society of America, 47, 967-974.

Wundt, W. (1859). Uber die Bewegungen der Augen. Verhandlungen des naturhistorischen-medizinischen. Vereins ze Heidelberg.

Wurtz, R.H., Goldberg, M.E., and Robinson, D.L. (1982). Brain mechanisms of visual attention. Scientific American, 246, 124-135.